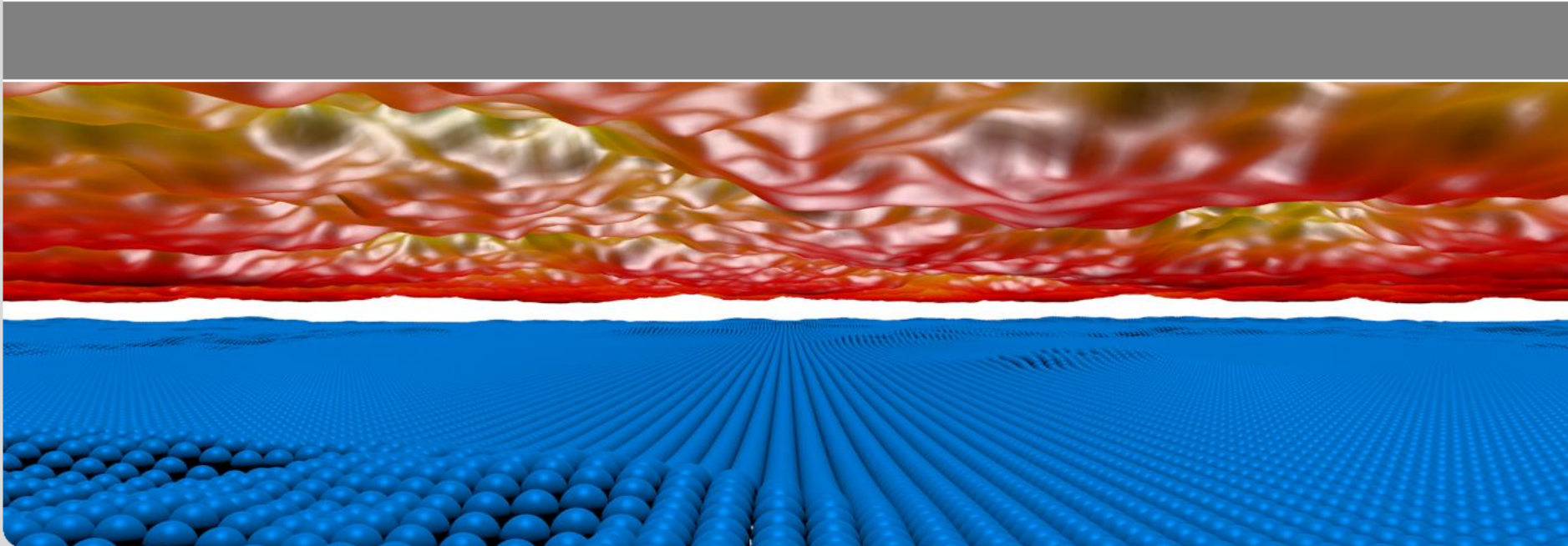


Contact mechanics

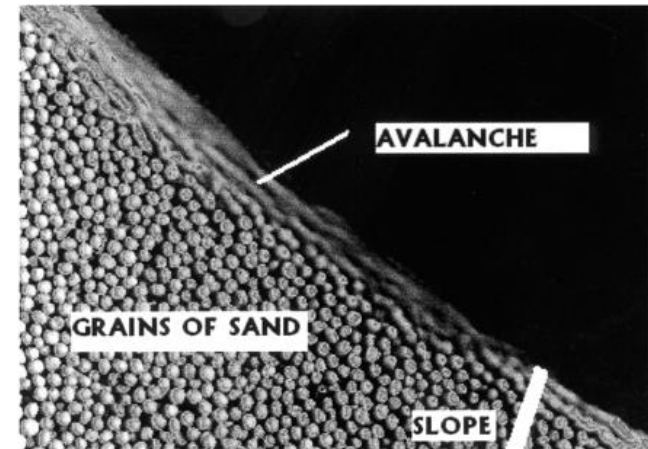
Lars Pastewka
Karlsruhe Institute of Technology



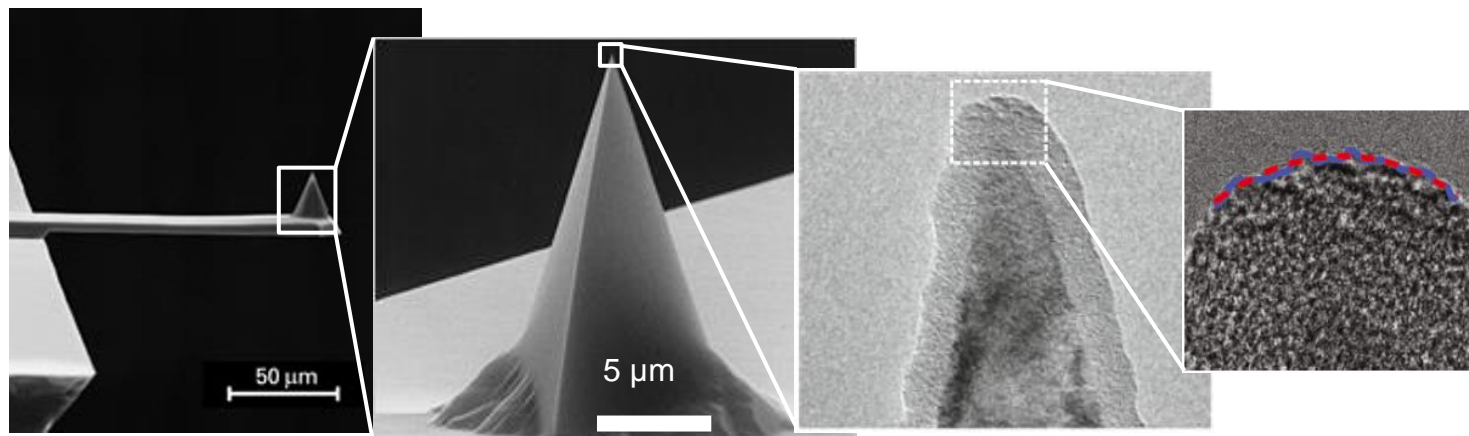
Contact mechanics



generalbearing.com



Scientific American



Schäfer, Greiner (KIT, IAM-CMS)

e.g. Jacobs et al., *Tribol. Lett.* (2013)

Outline

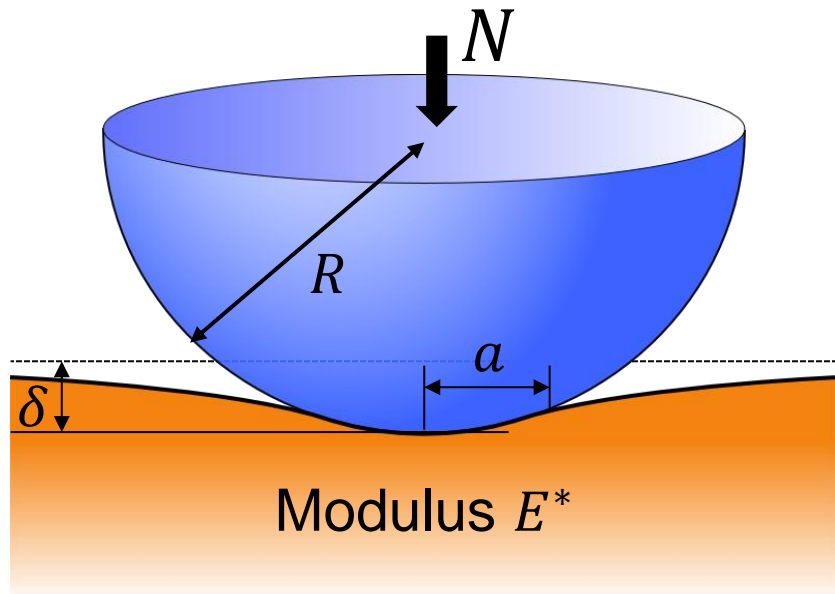
■ Contact of spheres

- Nonadhesive contact
- Adhesive contact
- Applications

■ Contact of rough surfaces

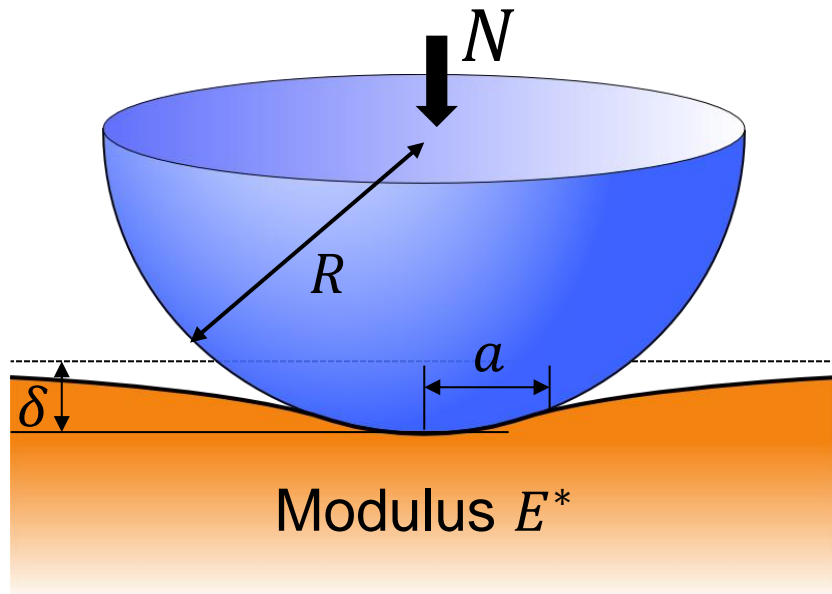
- Statistical description of rough surfaces
- Nonadhesive contact (incl. Greenwood-Williamson's and Persson's theories)
- Adhesive contact
- Applications

Elastic contact



Hertz (1881)

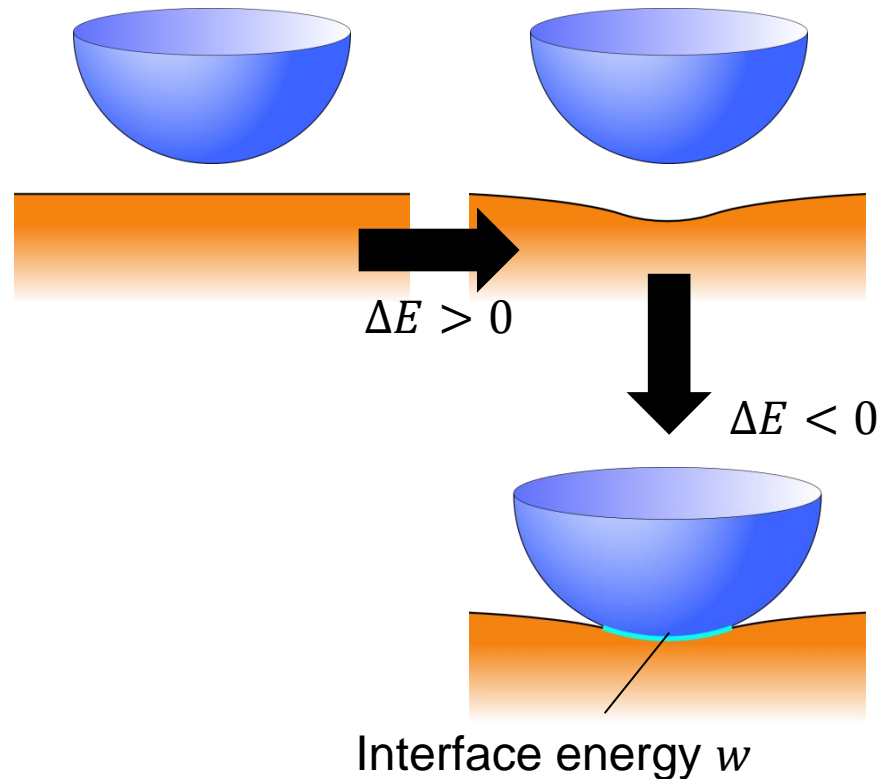
Elastic contact



Hertz (1881), JKR (1971),
 DMT (1975), Maugis-Dugdale (1992),

...

$$\frac{1}{E^*} = \frac{1 - \nu_1^2}{E_1} + \frac{1 - \nu_2^2}{E_2}$$



Hertz contact

Heinrich Hertz
1857-1894

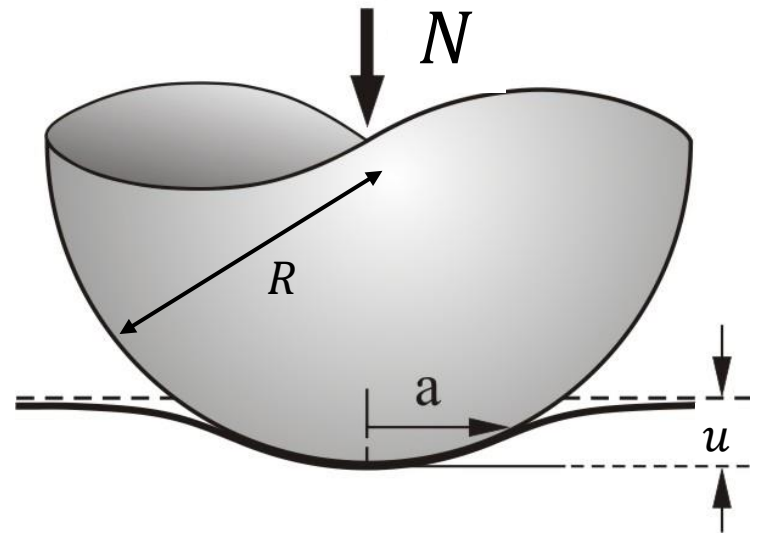


- Hertz contact $E^* = \frac{E}{1 - \nu^2}$
- Contact area A and displacement u

$$\frac{u}{R} = \frac{a^2}{R^2} = \frac{A}{\pi R^2} = \left(\frac{3}{4} \frac{N}{E^* R^2} \right)^{\frac{2}{3}}$$

- Contact stiffness $K = dN/du$

$$\frac{K}{E^* R} = \left(\frac{6N}{E^* R^2} \right)^{\frac{1}{3}} = \frac{2a}{R}$$



Ueber die Berührung fester elastischer Körper.

· (Von Herrn Heinrich Hertz.) J. reine angew. Math. 92, 156 (1881)

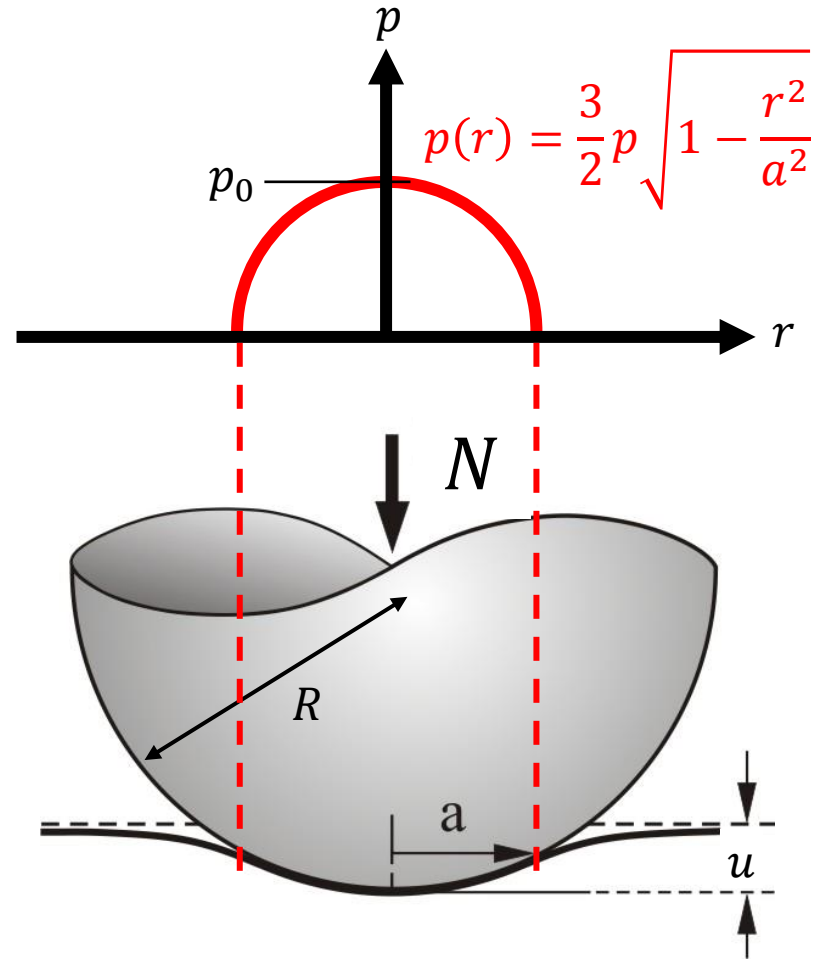
Hertz contact

- Hertz contact $E^* = \frac{E}{1 - \nu^2}$
- Contact area A and displacement u

$$\frac{u}{R} = \frac{a^2}{R^2} = \frac{A}{\pi R^2} = \left(\frac{3}{4} \frac{N}{E^* R^2} \right)^{\frac{2}{3}}$$

- Contact stiffness $K = dN/du$

$$\frac{K}{E^* R} = \left(\frac{6N}{E^* R^2} \right)^{\frac{1}{3}} = \frac{2a}{R}$$



Derivation?

- Green's functions: Boussinesq-Cerruti solution: Response to a concentrated force

$$\bar{u}_z = \frac{F}{\pi E^*} \frac{1}{r} \quad \rightarrow \quad G_{zz}(\vec{r}) = \frac{1}{\pi E^* |\vec{r}|}$$

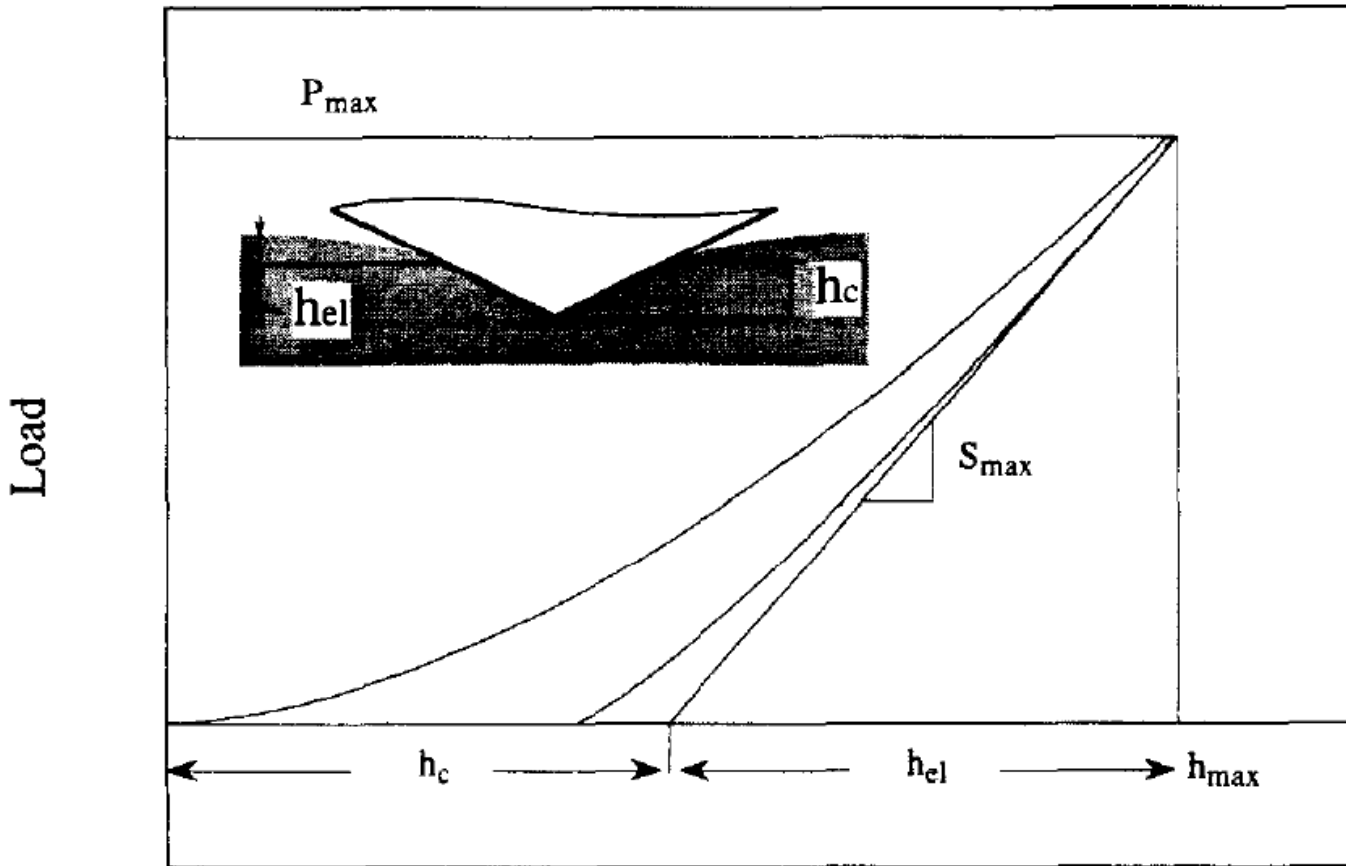
$$\frac{1}{E^*} = \frac{1 - \nu_1^2}{E_1} + \frac{1 - \nu_2^2}{E_2}$$

- Arbitrary pressure distributions: Convolution

$$\bar{u}_z(\vec{r}) = \int d^2 r' G_{zz}(\vec{r} - \vec{r}') p(\vec{r}')$$

- Typical derivation: Assume/guess $p(\vec{r})$

Indentation



Stiffness:

$$K = 2E^*a$$

Displacement

Fig. 1. Typical load–displacement plot for an indentation.

Vlassak, Nix, J. Mech. Phys. Solids
42, 1223-1245 (1994)

Indentation

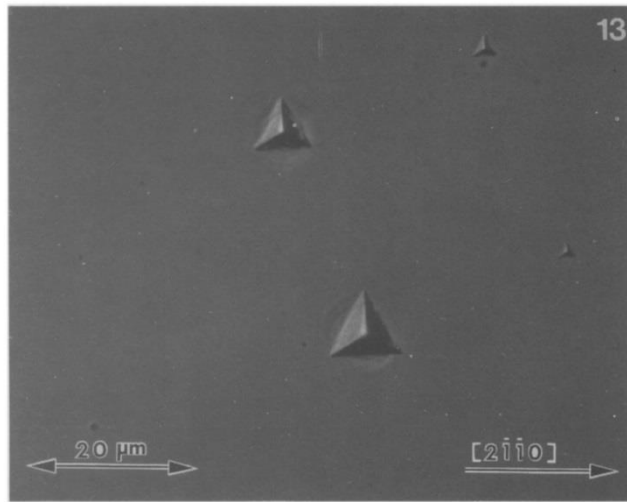


Fig. 13. Optical micrographs of indentations in a zinc single crystal. The surface of the sample is parallel to the basal plane.

Vlassak, Nix, J. Mech. Phys. Solids
42, 1223-1245 (1994)

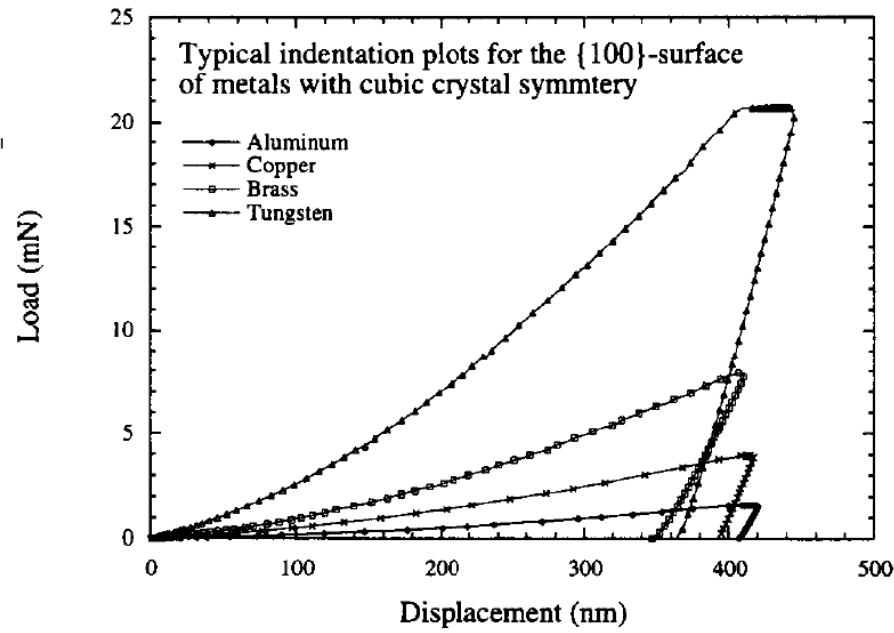
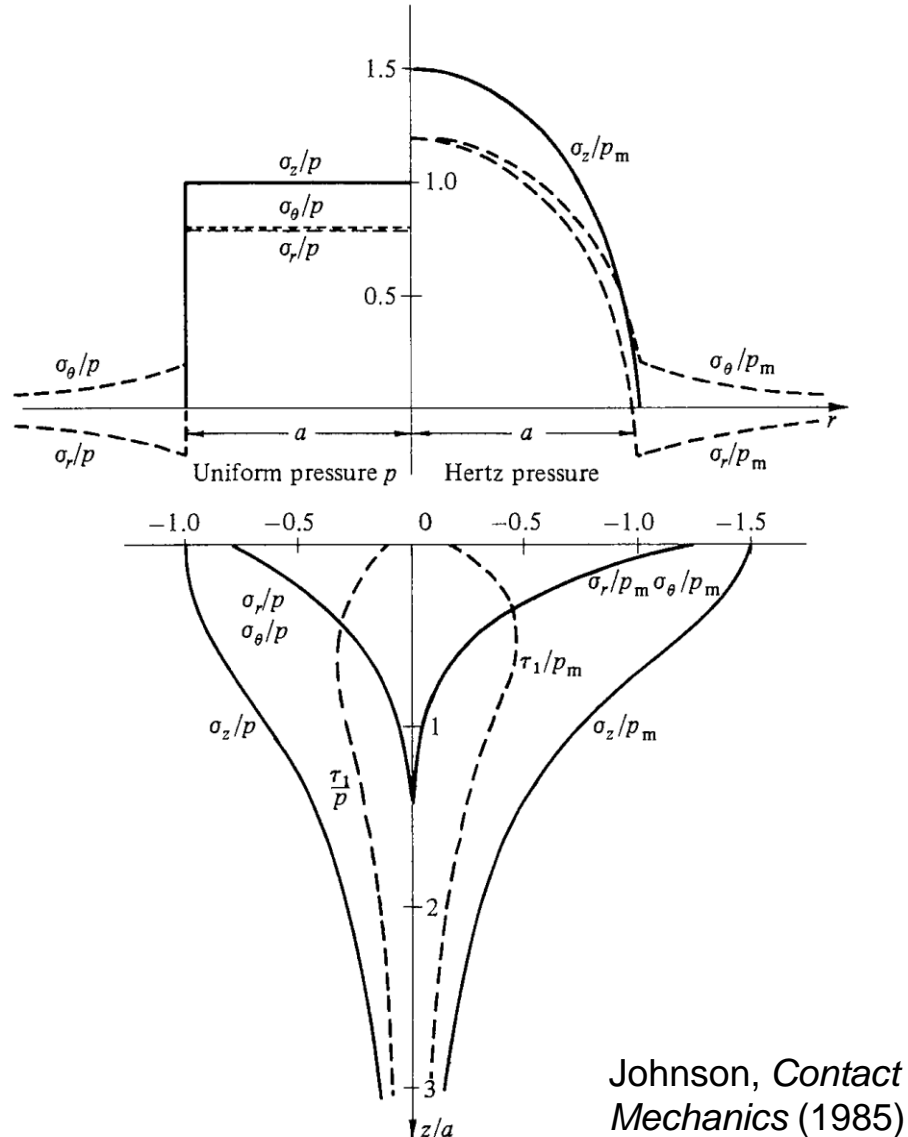


Fig. 6. Typical load-displacement curves for the {100} surfaces of the samples with cubic crystal symmetry. The loading cycles have been omitted for clarity.

Subsurface stress

Fig. 4.3. Stress distributions at the surface and along the axis of symmetry caused by (left) uniform pressure and (right) Hertz pressure acting on a circular area radius a .



Johnson, *Contact Mechanics* (1985)

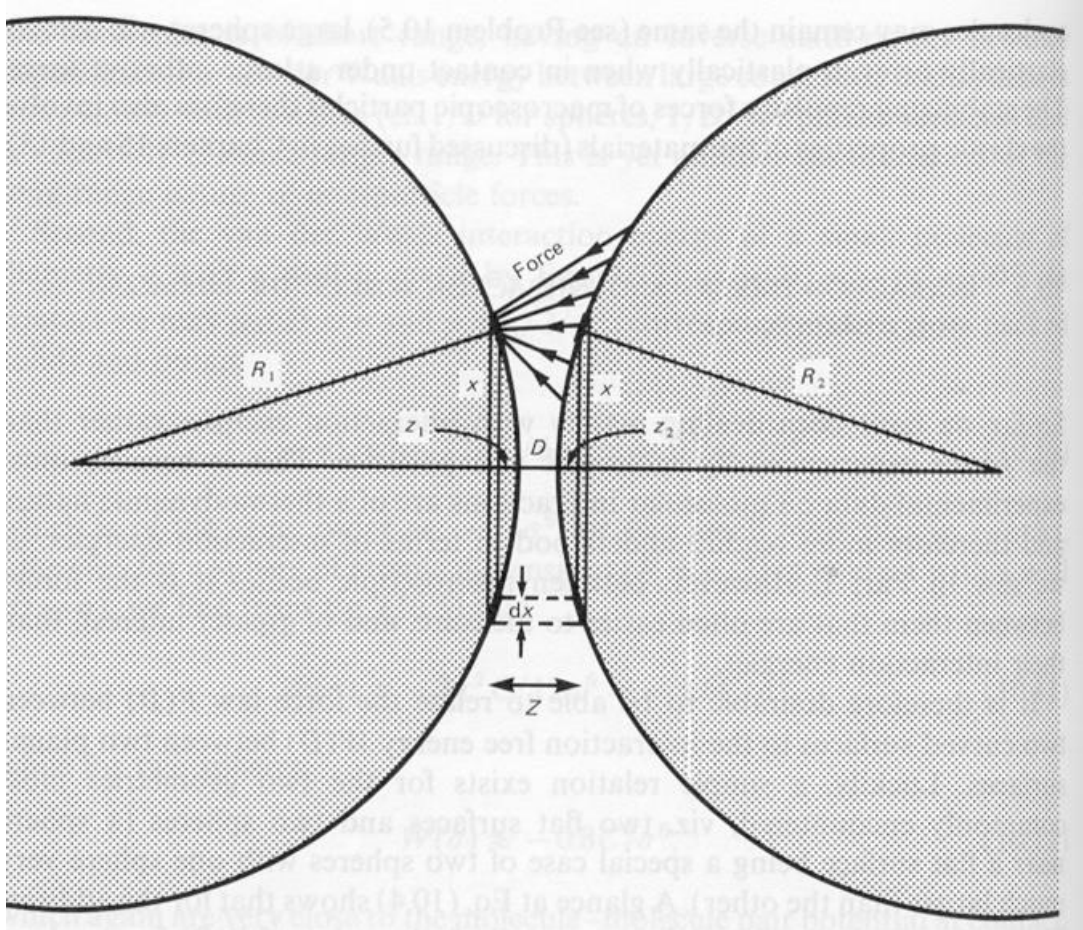
Adhesion: Intermolecular interactions

Type of interaction	Interaction energy $w(r)$
Covalent, metallic 	Complicated, short range
Charge-charge 	$Q_1 Q_2 / 4\pi\epsilon_0 r$ (Coulomb energy)
Charge-dipole 	$-Qu \cos \theta / 4\pi\epsilon_0 r^2$
Dipole-dipole 	$-Q^2 u^2 / 6(4\pi\epsilon_0)^2 k T r^4$ $-u_1 u_2 [2 \cos \theta_1 \cos \theta_2 - \sin \theta_1 \sin \theta_2 \cos \phi] / 4\pi\epsilon_0 r^3$ $-u_1^2 u_2^2 / 3(4\pi\epsilon_0)^2 k T r^6$ (Keesom energy)
Charge-non-polar 	$-Q^2 \alpha / 2(4\pi\epsilon_0)^2 r^4$
Dipole-non-dipolar 	$-u^2 \alpha (1 + 3 \cos^2 \theta) / 2(4\pi\epsilon_0)^2 r^6$ $-u^2 \alpha / (4\pi\epsilon_0)^2 r^6$ (Debye energy)
Two non-polar molecules 	$\frac{3}{4} \frac{h v \alpha^2}{(4\pi\epsilon_0)^2 r^6}$ (London dispersion energy)
Hydrogen bond 	Complicated, short range, energy roughly proportional to $-1/r^2$

From:
Israelachvili,
Intermolecular & Surface Forces (1991)
p. 28

Fig. 2.2. Common types of interactions between atoms, ions and molecules in vacuum. $w(r)$ is the interaction free energy (in J); Q , electric charge (C); u , electric dipole moment ($C \cdot m$); α , electric polarizability ($C^2 \cdot m^2 \cdot J^{-1}$); r , distance between interacting atoms or molecules (m); k , Boltzmann constant ($1.381 \times 10^{-23} \text{ J K}^{-1}$); T , absolute temperature (K); h , Planck's constant ($6.626 \times 10^{-34} \text{ Js}$); v , electronic absorption (ionization) frequency (s^{-1}); ϵ_0 , dielectric permittivity of free space ($8.854 \times 10^{-12} \text{ C}^2 \text{ J}^{-1} \text{ m}^{-1}$). The force is obtained by differentiating the energy $w(r)$ with respect to distance r .

Derjaguin approximation



$$F(D) = 2\pi R w_{\text{flat}}(D)$$

From Israelachvili, Intermolecular & Surface Forces

Derjaguin approximation

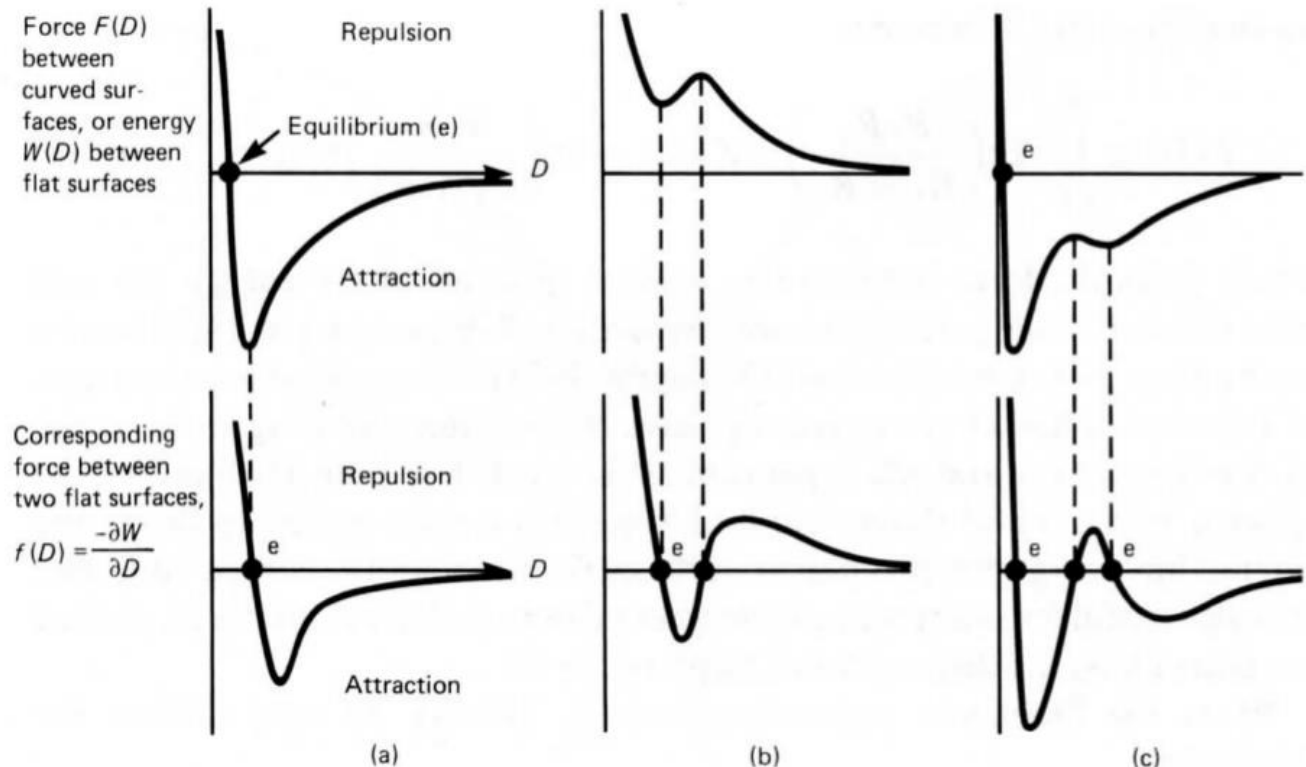
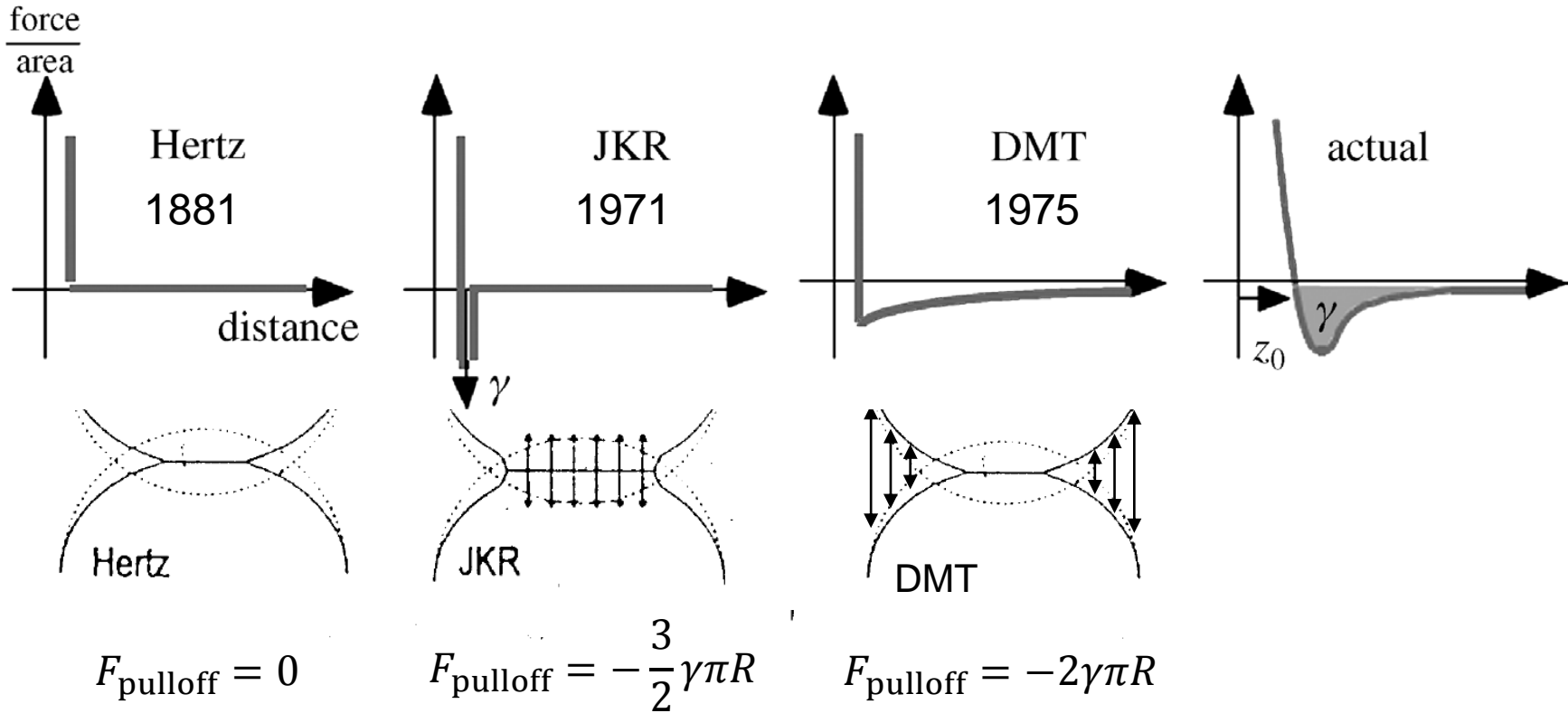
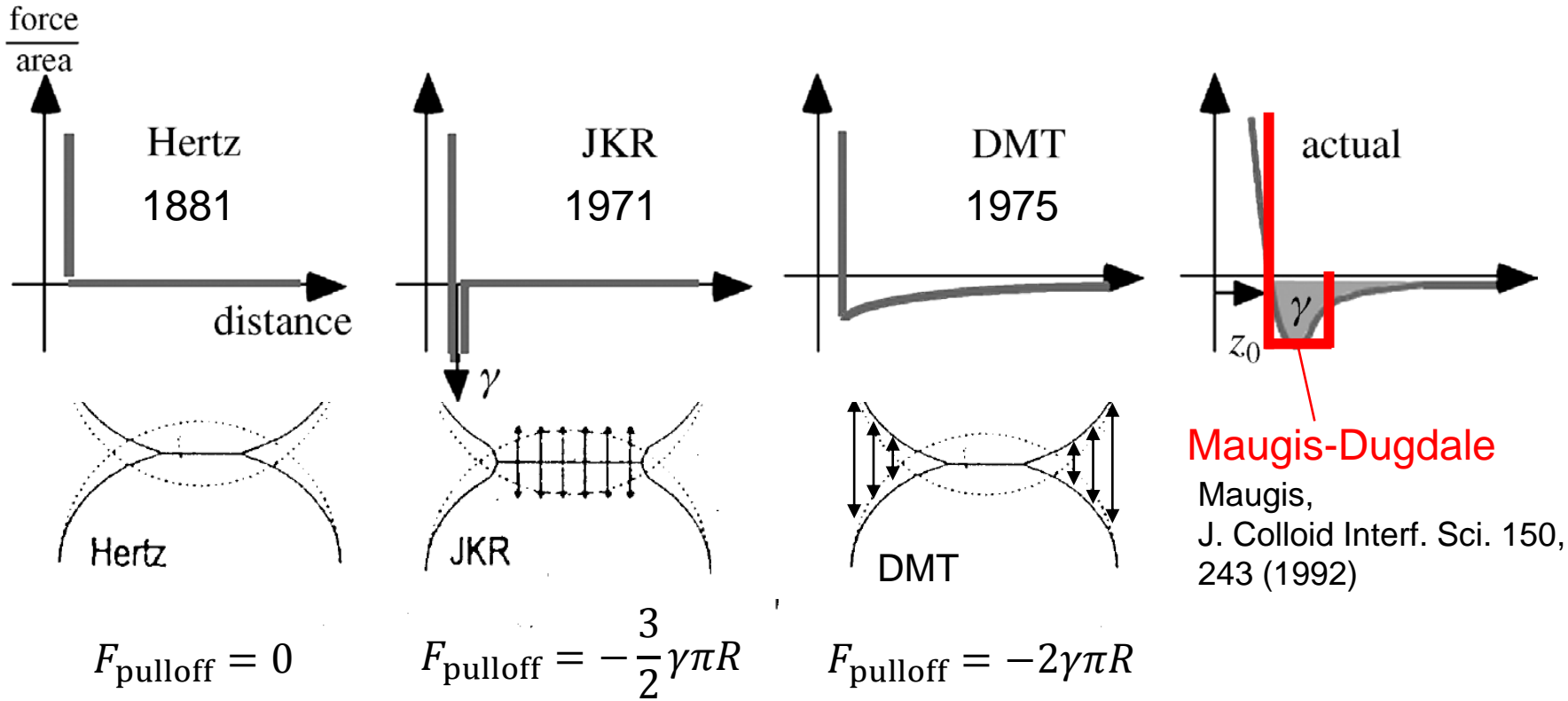


Fig. 10.4. Top row: force laws between two curved surfaces (e.g., two spherical particles). Bottom row: corresponding force laws between two flat surfaces. Note that stable equilibrium occurs only at points marked e where the force is zero ($f = 0$) and the force curve has negative slope; the other points where $f = 0$ are unstable.

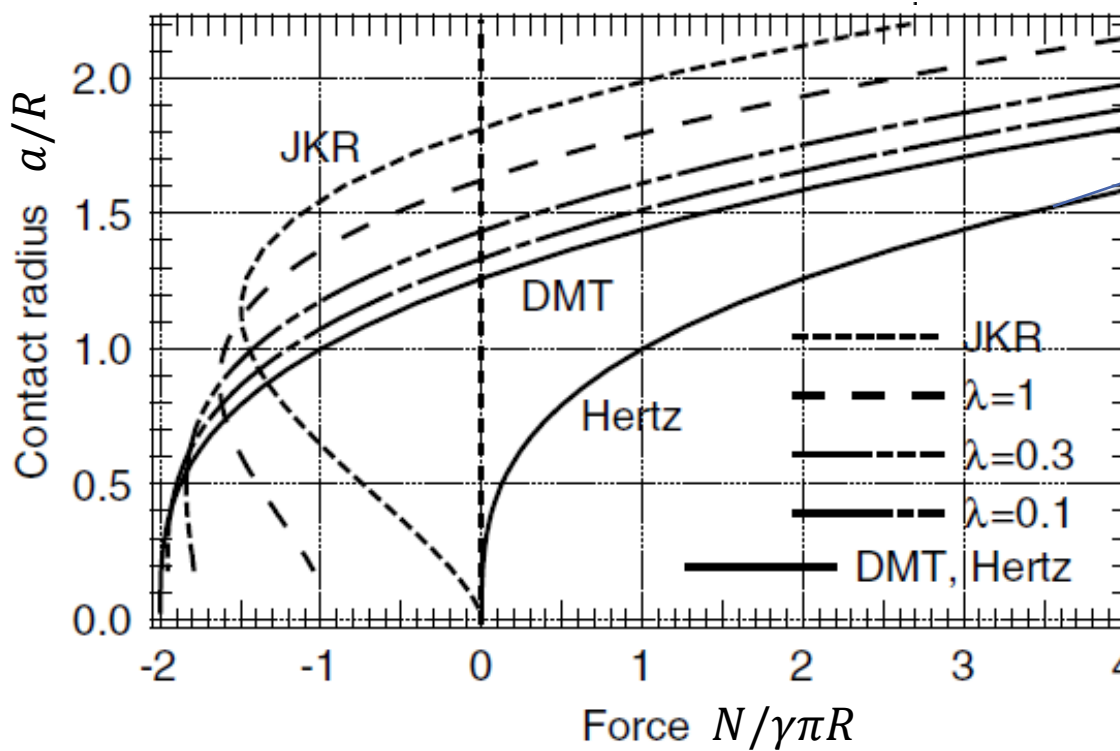
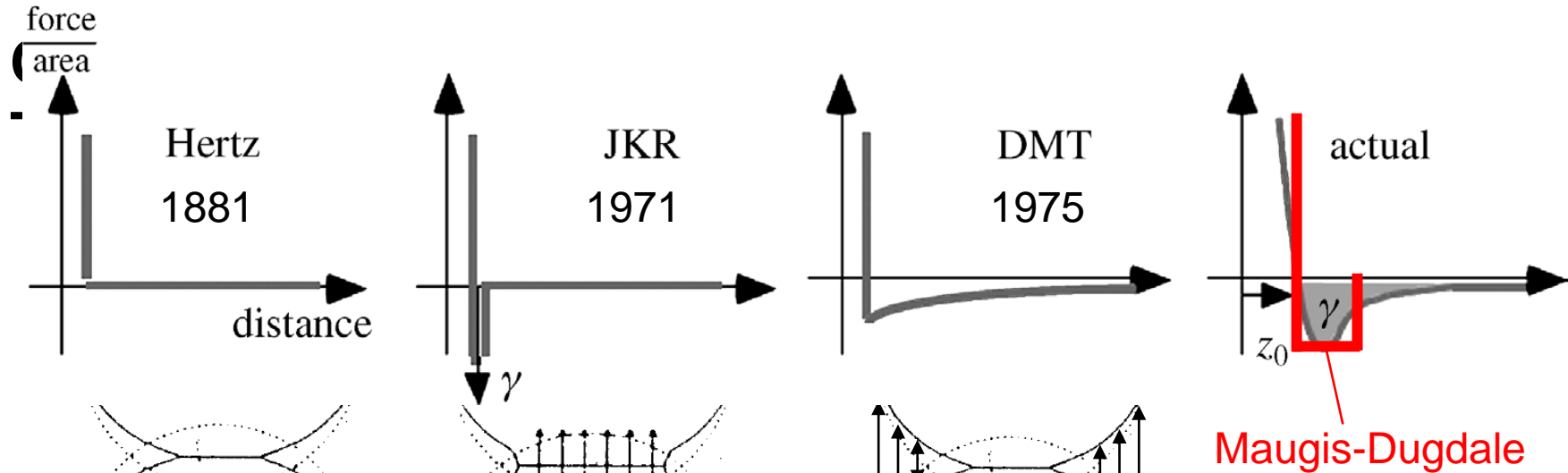
From:
 Israelachvili,
Intermolecular & Surface Forces (1991), p. 164



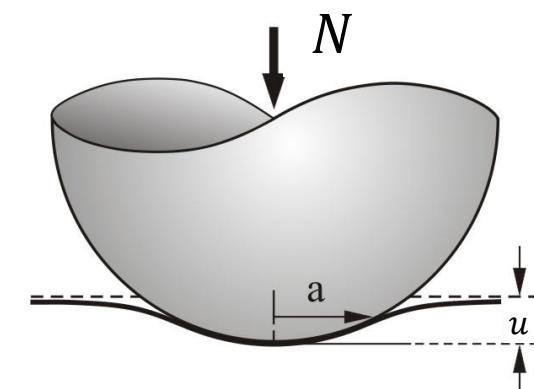
JKR = Johnson-Kendall-Roberts
DMT = Derjaguin-Muller-Toporov



JKR = Johnson-Kendall-Roberts
DMT = Derjaguin-Muller-Toporov



$$\text{Hertz: } a \propto N^{1/3}$$



Direct Measurement of Interfacial Interactions between Semispherical Lenses and Flat Sheets of Poly(dimethylsiloxane) and Their Chemical Derivatives

Manoj K. Chaudhury*,† and George M. Whitesides*,‡

Dow Corning Corporation, Midland, Michigan 48686, and Department of Chemistry,
Harvard University, Cambridge, Massachusetts 02138

Received May 5, 1990. In Final Form: September 20, 1990

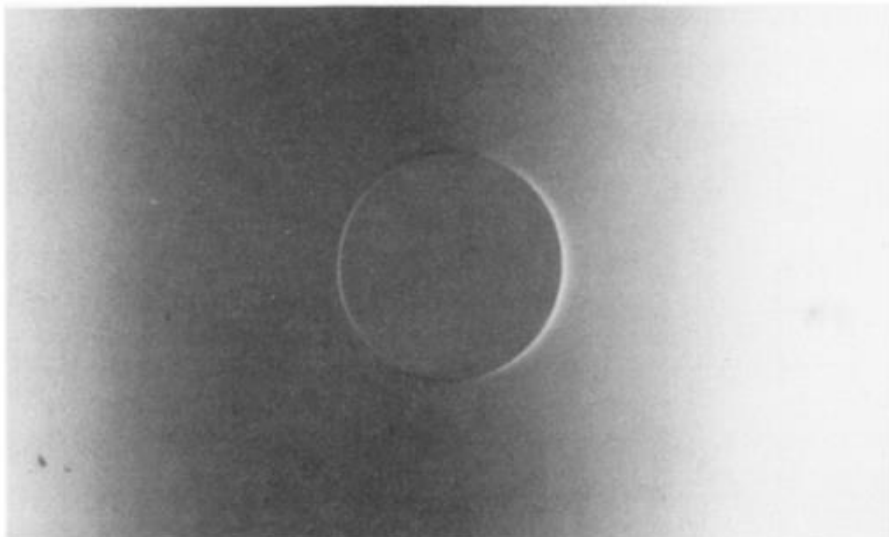


Figure 3. Photomicrograph showing the contact area (radius = 154 μm) resulting from the contact (in air) between a lens ($R = 1.44 \text{ mm}$) and a flat sheet of PDMS. The edge of the lens is outside the field of view. There was no external load on the lens and hence the deformation was solely due to the effect of surface forces.

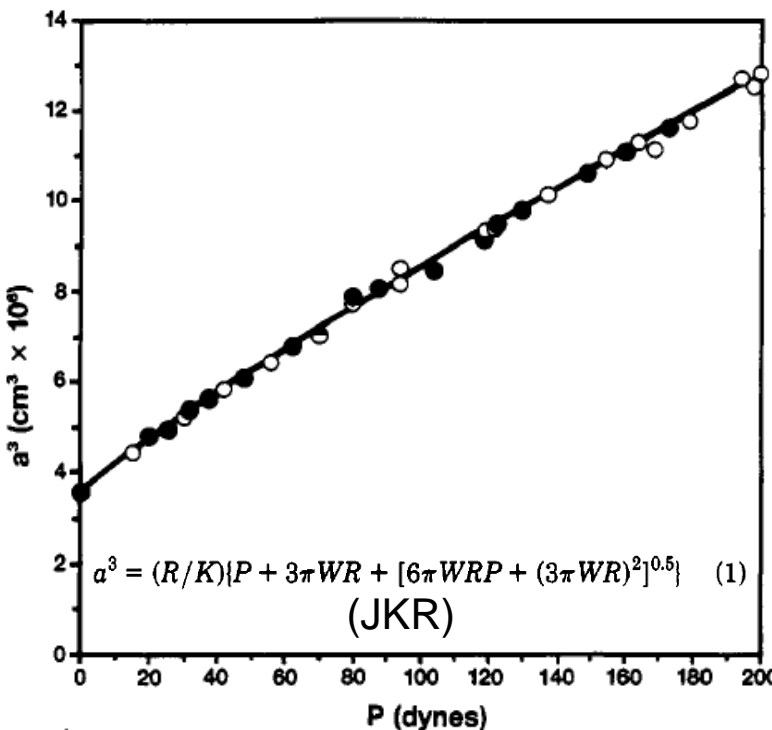
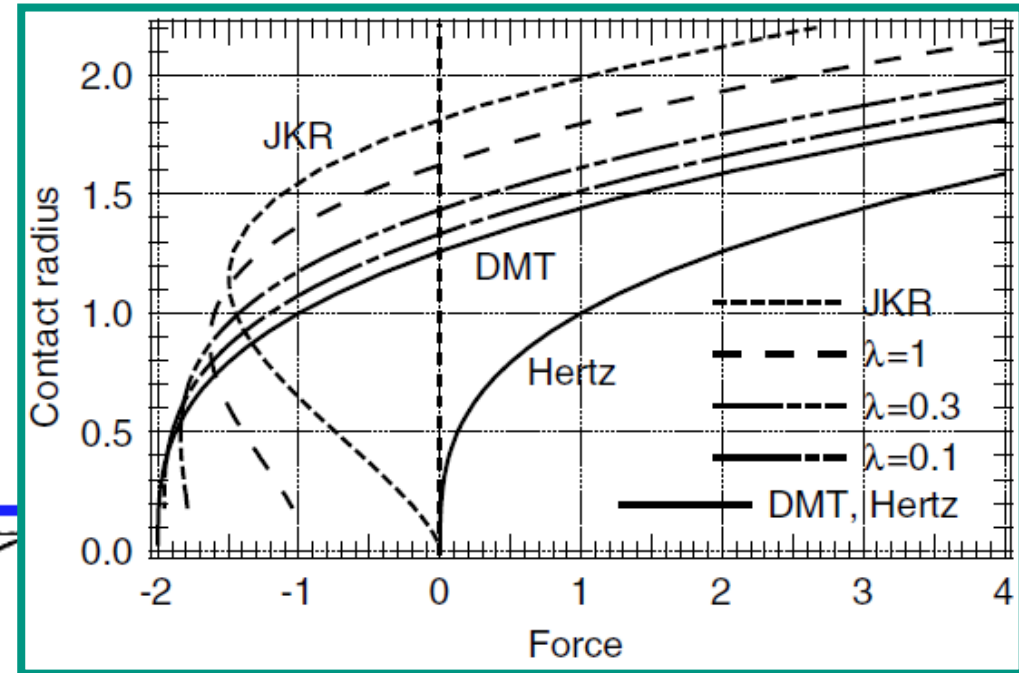
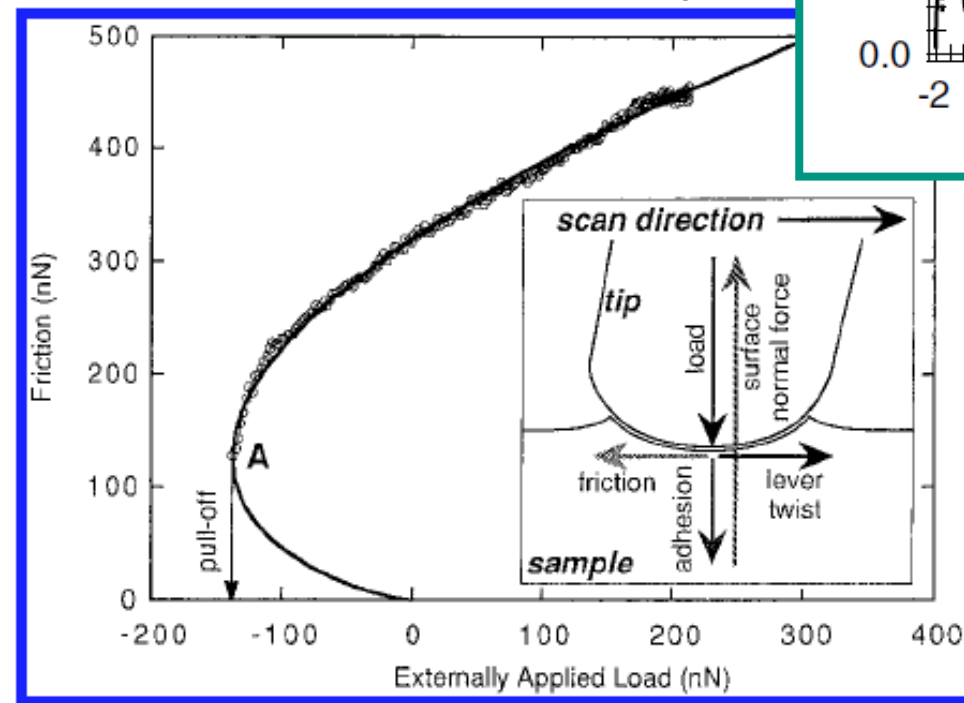


Figure 4. Plot of a^3 against P following the form expected from eq 1. The data were obtained from the load-deformation experiments using unmodified PDMS. The radius of the lens used in these measurements was 1.44 mm. The open circles (\circ) represent the data obtained from increasing loads and the closed circles (\bullet) represent the data obtained from decreasing loads: there is no hysteresis. The solid line was obtained from the analysis of these data by using eq 1.

Friction force microscopy

Platinum-coated tip on mica



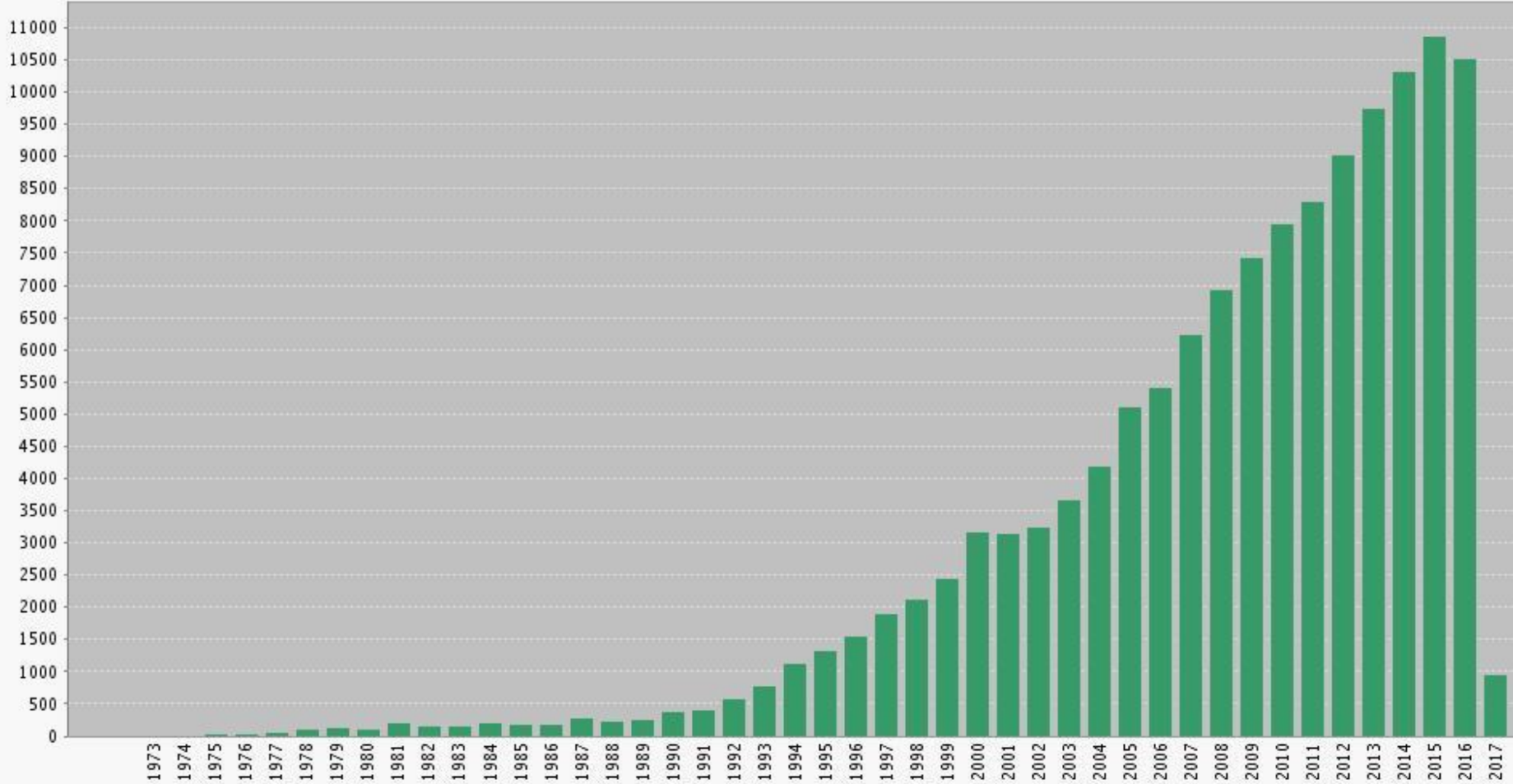
- Idea: Constant shear strength τ of interface

$$F = \tau A = \tau \pi a^2$$

- Area from JKR

Carpick, Agrait, Ogletree, Salmeron, Langmuir 12, 3334 (1996)

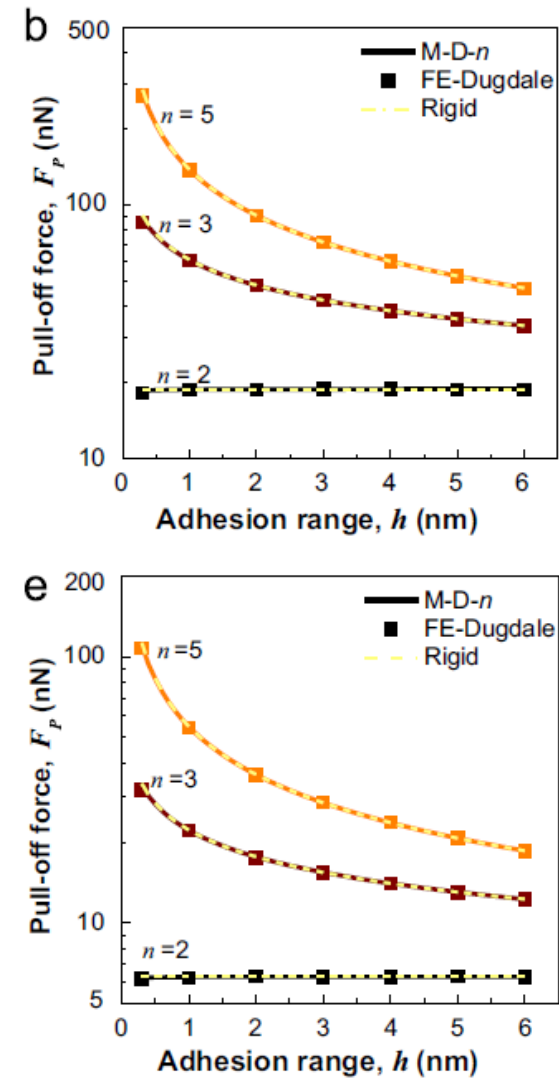
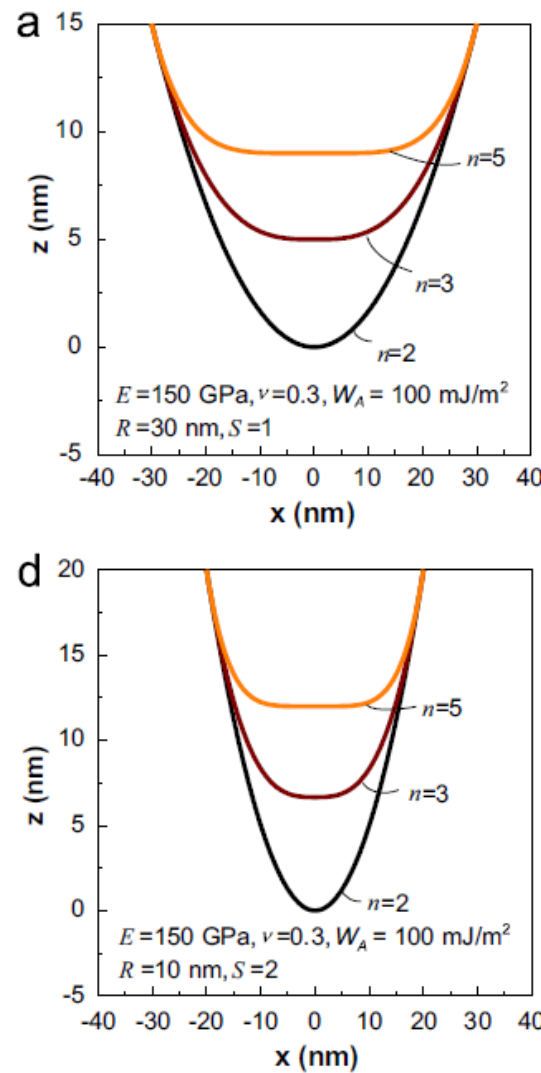
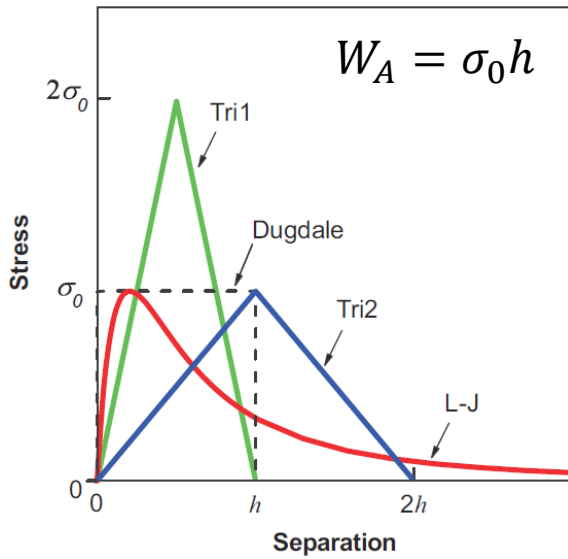
Citations to JKR/DMT



Power-law indenter

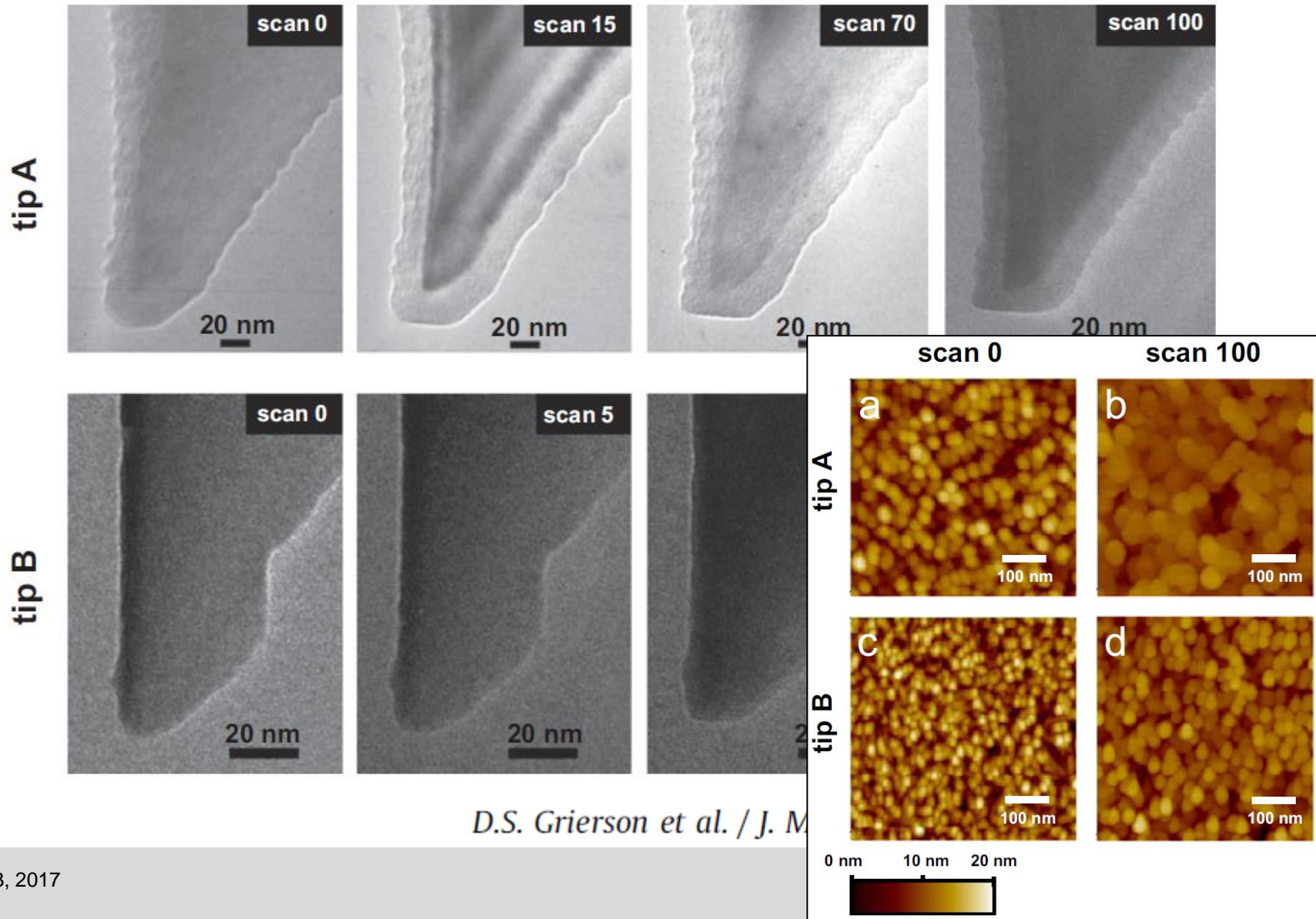
$$z(r) = \frac{r^n}{nQ}$$

$$F_{p-r \text{ Dug}} = \frac{W_A}{h} \pi (nhQ)^{2/n}$$



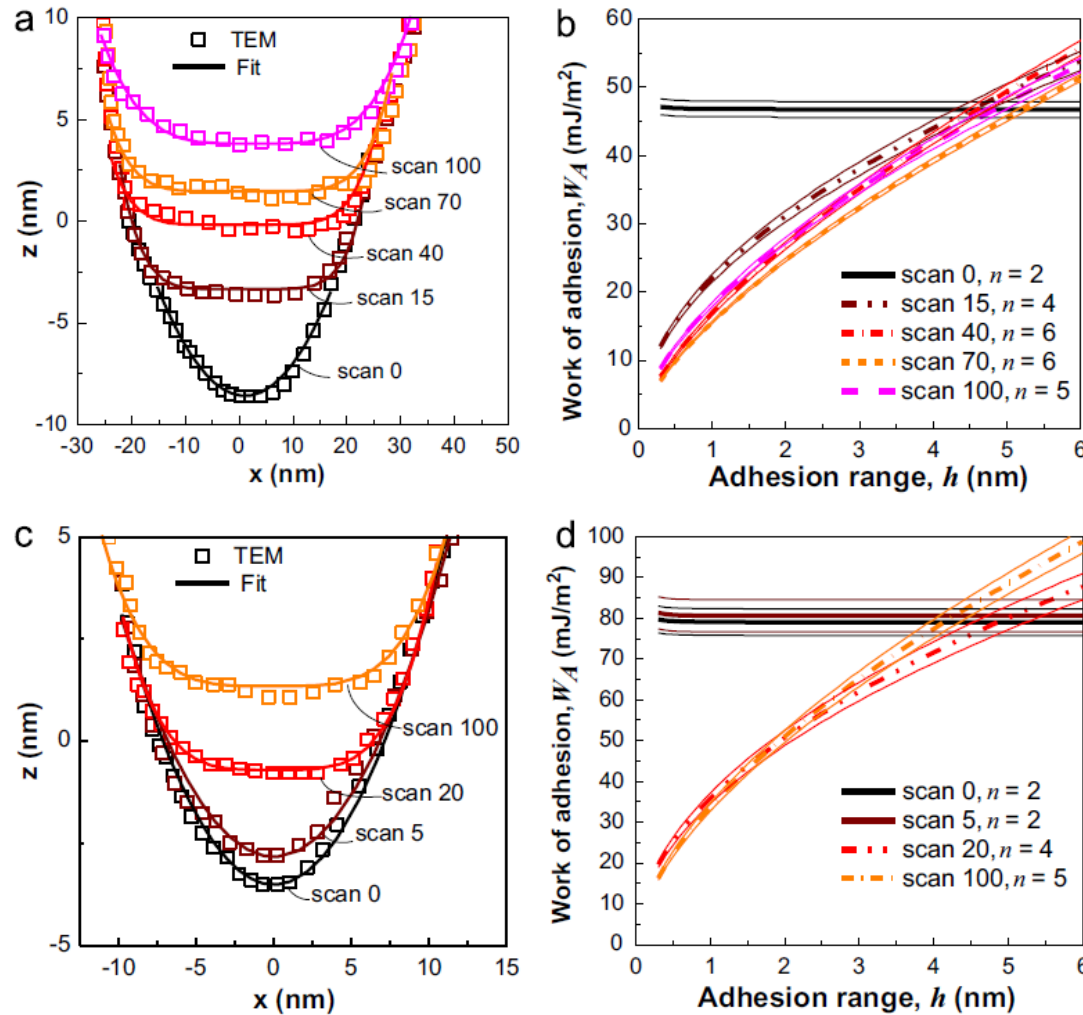
D.S. Grierson et al. / J. Mech. Phys. Solids 61 (2013) 597–610

Power-law indenter



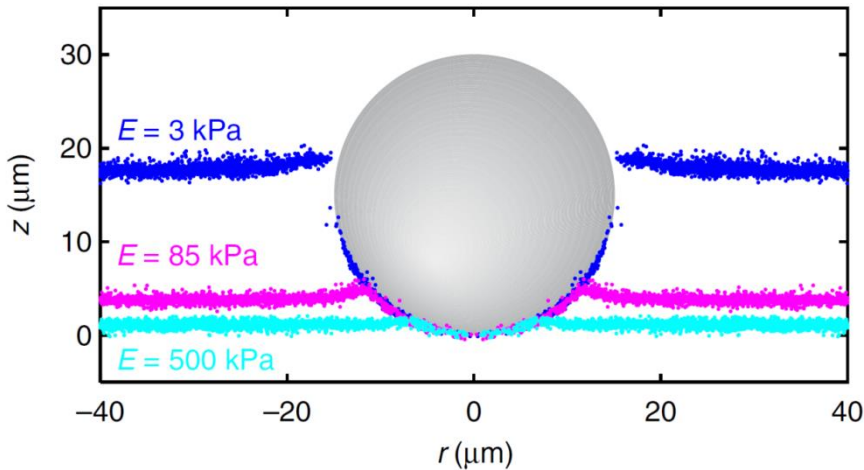
D.S. Grierson et al. / J. M.

Power-law indenter



D.S. Grierson et al. / J. Mech. Phys. Solids 61 (2013) 597–610

Soft solids



Silikon unterschiedlicher
Vernetzung zur
Steuerung von E

ARTICLE

Received 16 Sep 2013 | Accepted 8 Oct 2013 | Published 7 Nov 2013

DOI: 10.1038/ncomms3728

Surface tension and contact with soft elastic solids

Robert W. Style¹, Callen Hyland¹, Rostislav Boltyanskiy¹, John S. Wettlaufer^{1,2} & Eric R. Dufresne¹

Nature Communications 4, 2728 (2013)

Mar. 03, 2017

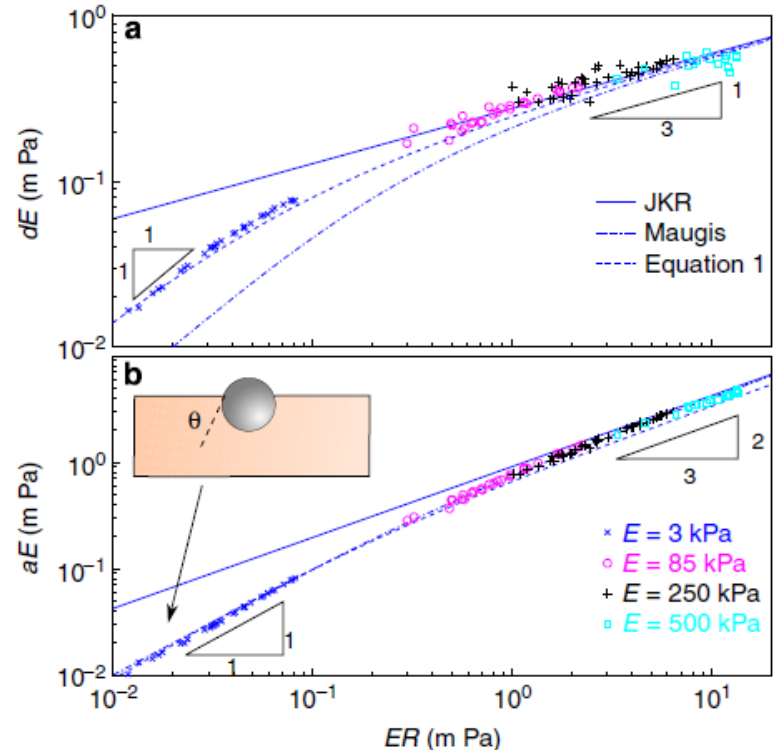


Figure 3 | Collapse of indentation data. (a) Indentation \times Young's modulus versus bead radius \times Young's modulus. (b) Contact radius \times Young's modulus versus bead radius \times Young's modulus. Inset: schematic of particle behaviour for $ER \ll 1$. For both quantities, the data collapses on a smooth curve. The dotted line shows the best-fit JKR theory¹³. The dash-dotted curve shows Maugis's extended JKR predictions⁴³. The dashed curve is derived from equation 2. Points show measured data for substrates with stiffness 3 kPa (blue), 85 kPa (magenta), 250 kPa (black) and 500 kPa (cyan).

From micro to nano contacts in biological attachment devices

Eduard Arzt^{†‡}, Stanislav Gorb^{†§}, and Ralph Spolenak[†]

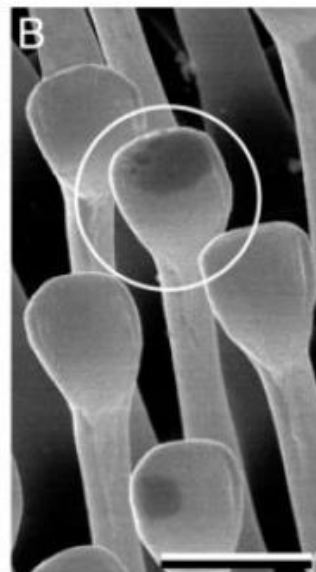
[†]Max Planck Institute for Metals Research, Heisenbergstrasse 3, 70569 Stuttgart, Germany; and [§]Biological Microtribology Group, Max Planck Institute of Developmental Biology, Spemannstrasse 35, 72076 Tübingen, Germany

PNAS | September 16, 2003 | vol. 100 | no. 19 | 10603–10606

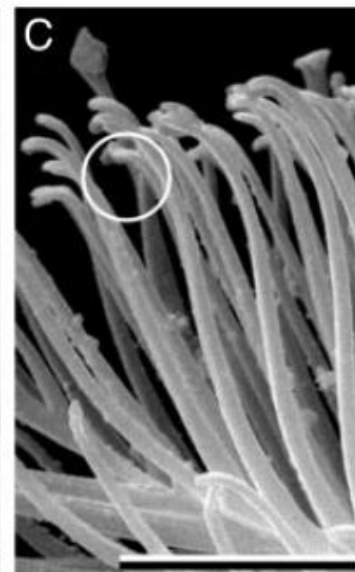
body mass →



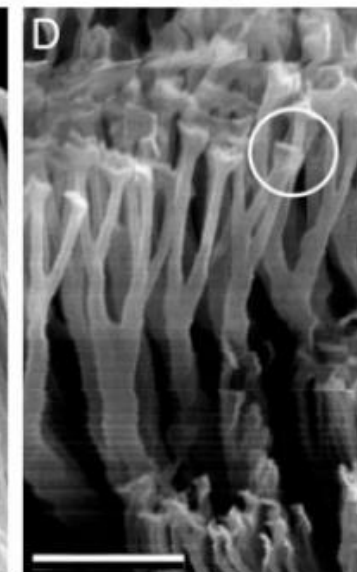
beetle



fly



spider



gecko

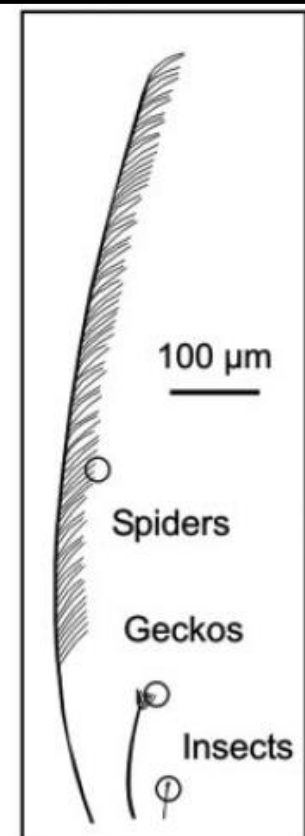


Fig. 1. Terminal elements (circles) in animals with hairy design of attachment pads. Note that heavier animals exhibit finer adhesion structures.

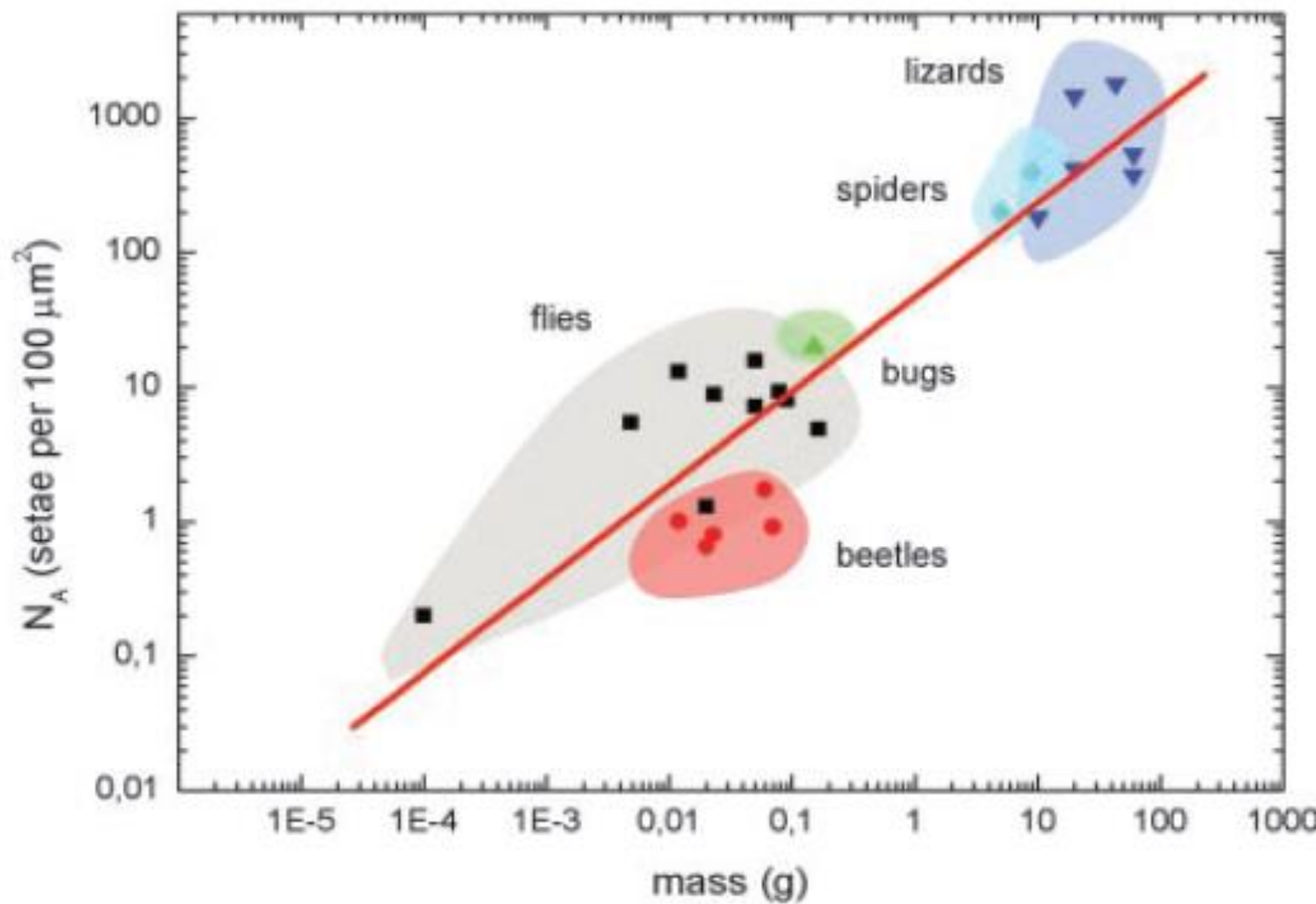


Fig. 2. Dependence of the terminal element density (N_A) of the attachment pads on the body mass (m) in hairy-pad systems of diverse animal groups ($\log \cdot N_A(m^{-2}) = 13.8 + 0.699 \cdot \log \cdot m(kg)$, $R = 0.919$).

Fibrillar adhesion

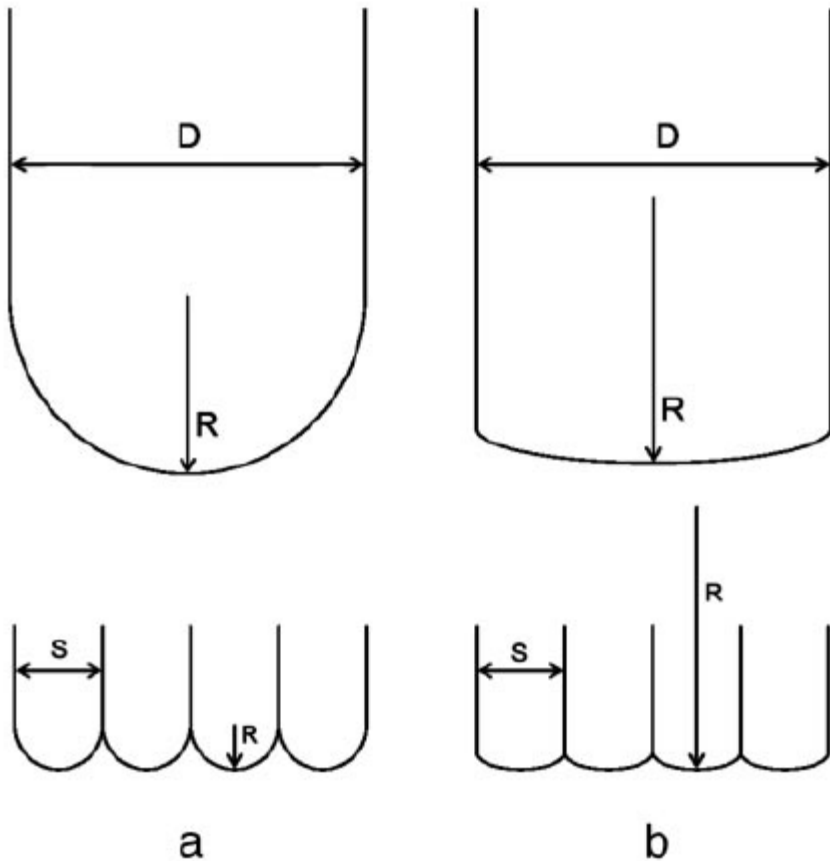


Fig. 4. Two cases of contact scaling. (a) Self-similarity: contact radius R scales with contact size s . (b) Curvature invariance: contact radius is independent of contact size.

- Mass mass density
 $m = D^3 \rho p$ ← shape factor
- Adhesion force safety factor
 $F_W = k mg$
- Areal density of setae
 $N_A = \frac{n}{D^2} = \frac{1}{s^2}$ number of setae
- Radius scales with setae diameter
 $F_C = n \frac{3}{2} \pi s w = \frac{3}{2} \pi D^2 w \sqrt{N_A}$
- Constant radius
 $N_A \propto m^{2/3}$
- Constant radius
 $N_A \propto m^{1/3}$

Fibrillar adhesion

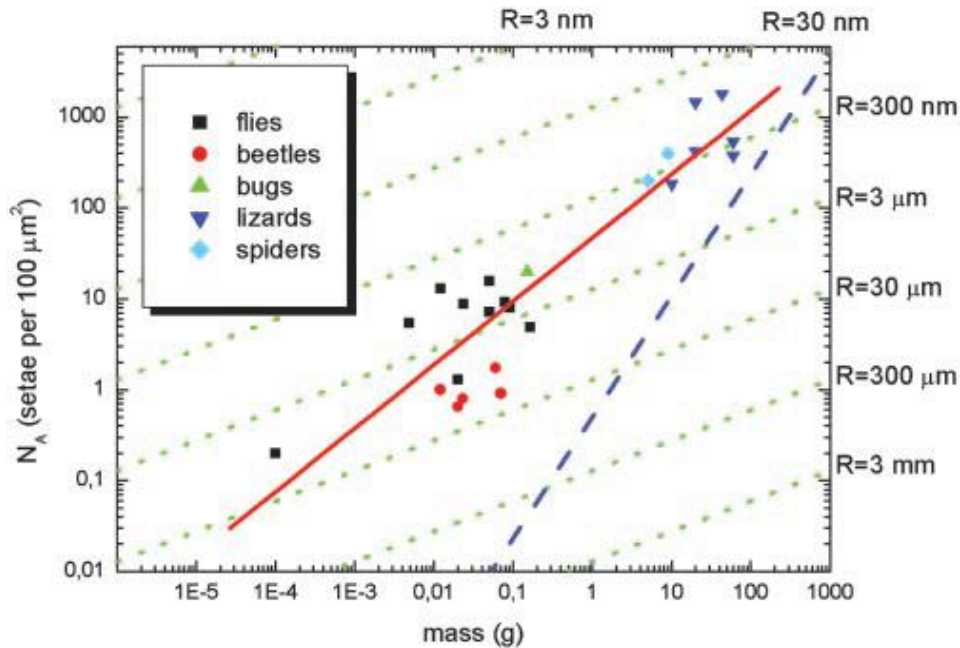
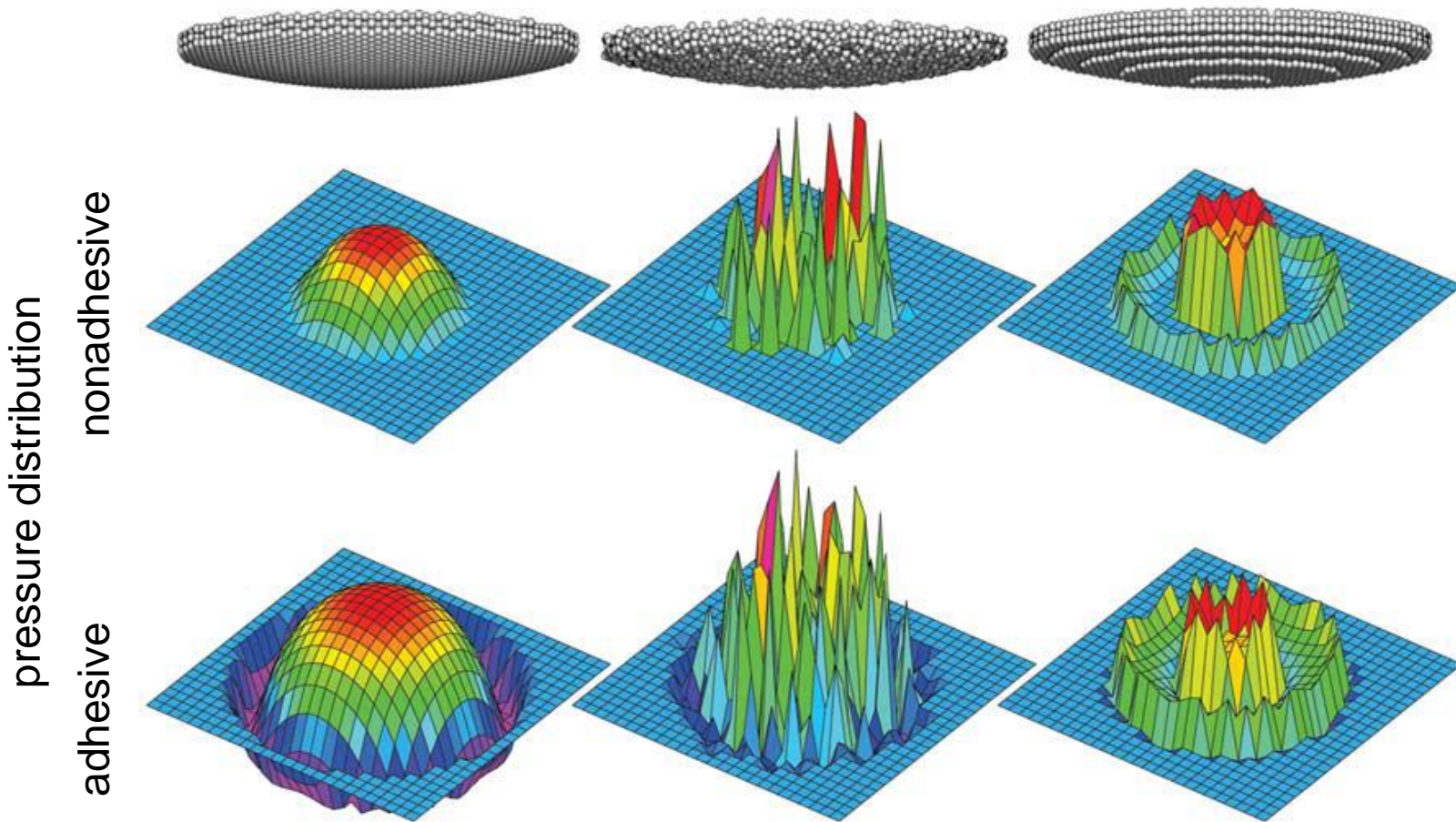


Fig. 3. Interpretation of Fig. 2 in light of contact theory. A fit to all data (red line) gives a slope of $\approx 2/3$, corresponding to the self-similarity criterion. Within each lineage, a lower slope of $\approx 1/3$ is found, suggesting curvature invariance of the contacts with radius R (green lines). The approximate limit for such attachment devices (limit of maximum contact) is shown as a blue line.

- Mass
 - $m = D^3 \rho p$ ← shape factor
- Adhesion force
 - $F_W = kmg$ ← safety factor
- Areal density of setae
 - $N_A = \frac{n}{D^2} = \frac{1}{s^2}$
 - number of setae
- Radius scales with setae diameter
 - $F_C = n \frac{3}{2} \pi s w = \frac{3}{2} \pi D^2 w \sqrt{N_A}$
 - $N_A \propto m^{2/3}$
- Constant radius
 - $N_A \propto m^{1/3}$

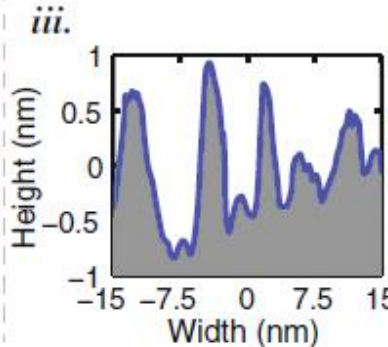
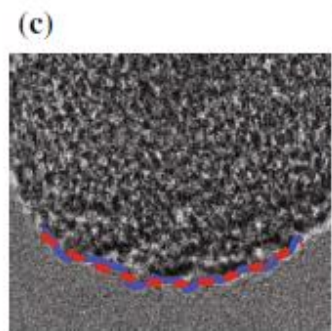
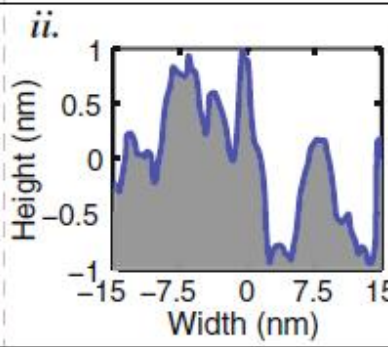
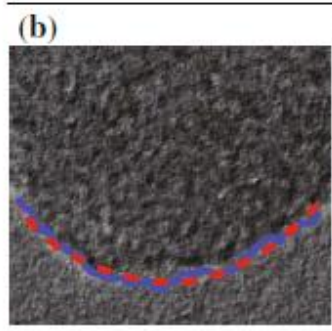
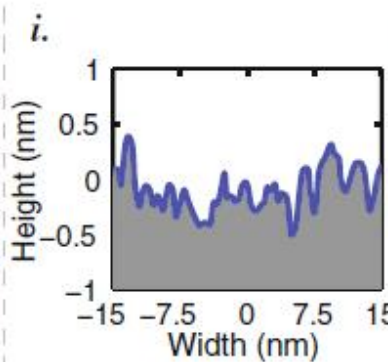
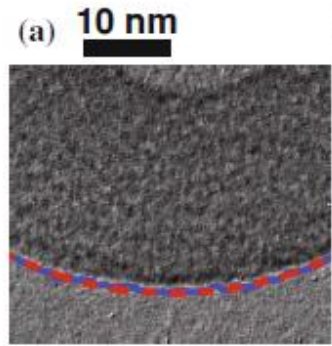
Roughness

Surface roughness

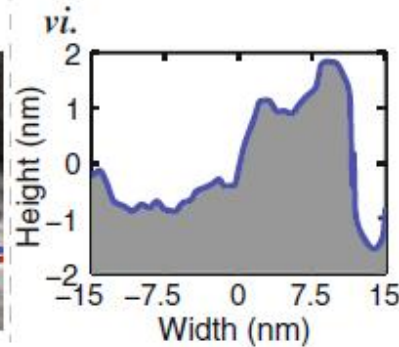
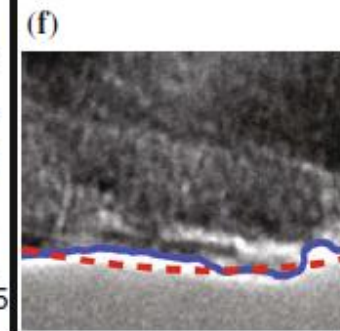
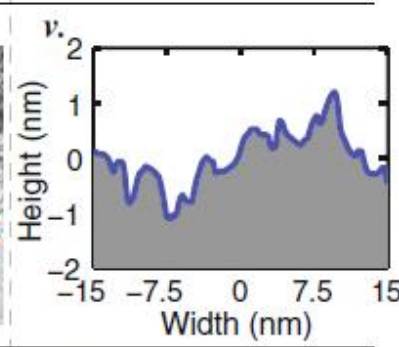
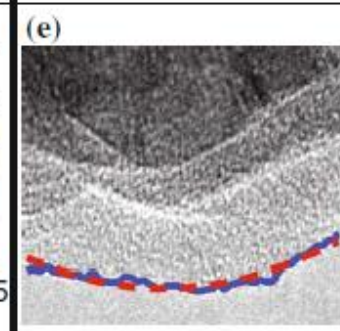
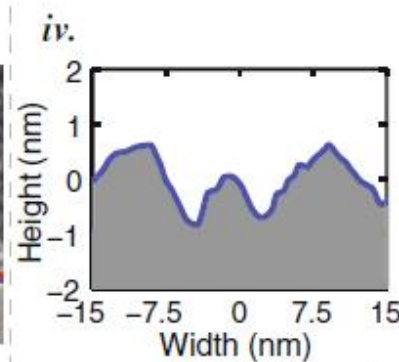
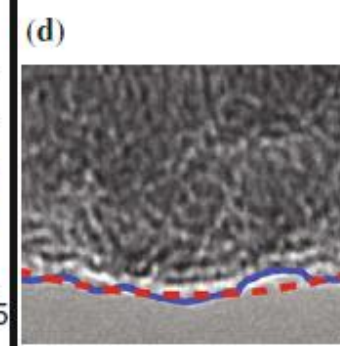


Luan, Robbins, Nature 435, 929 (2005)

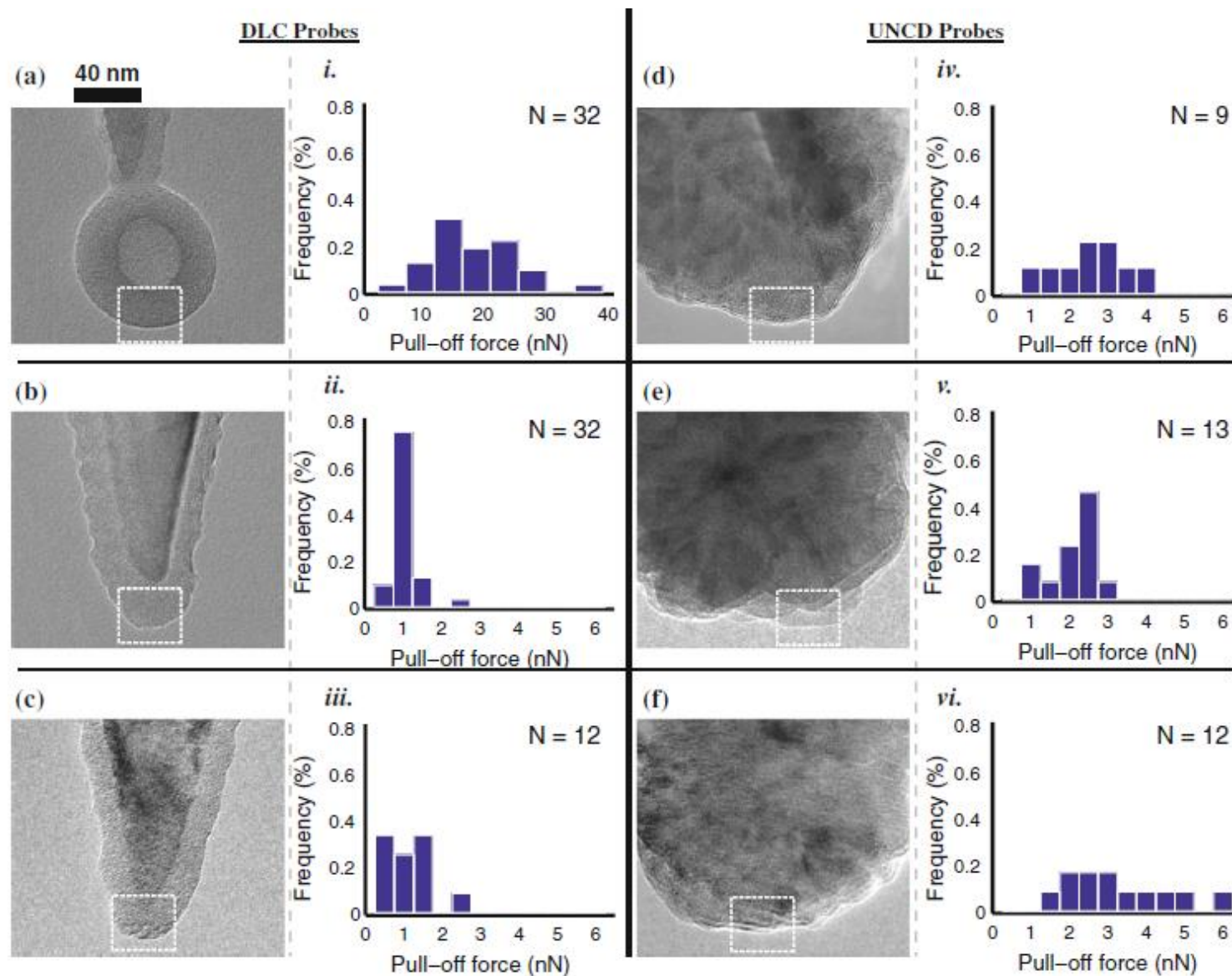
DLC Probes



UNCD Probes

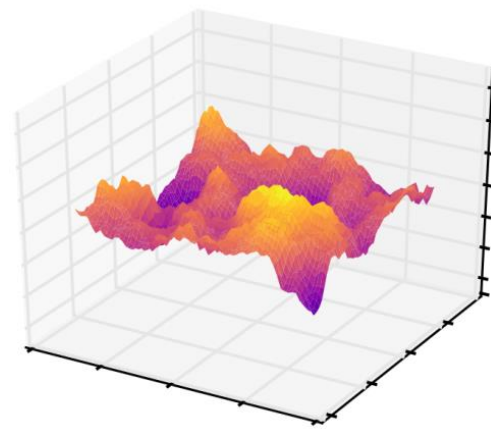
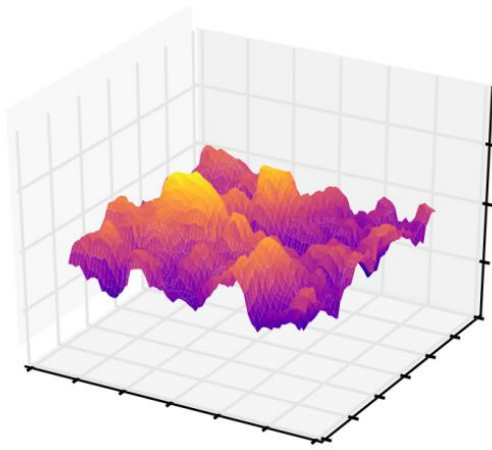
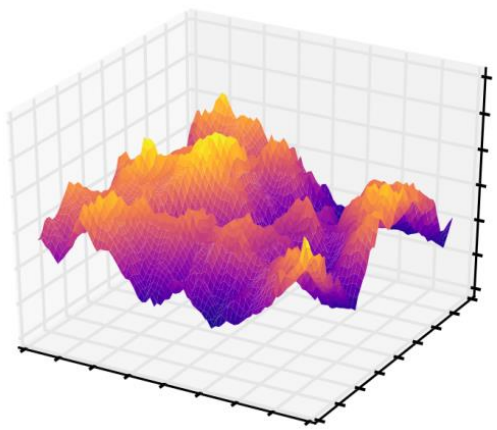


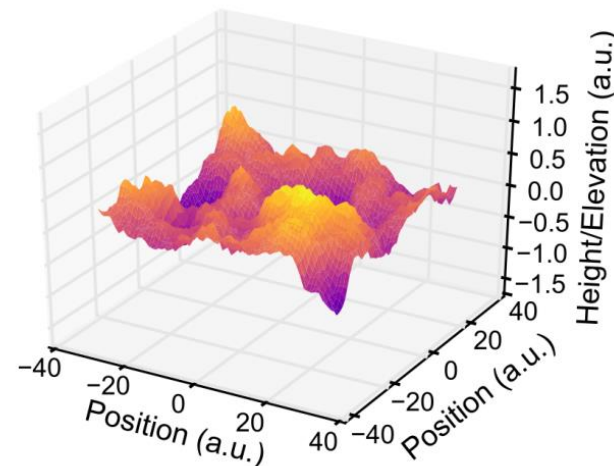
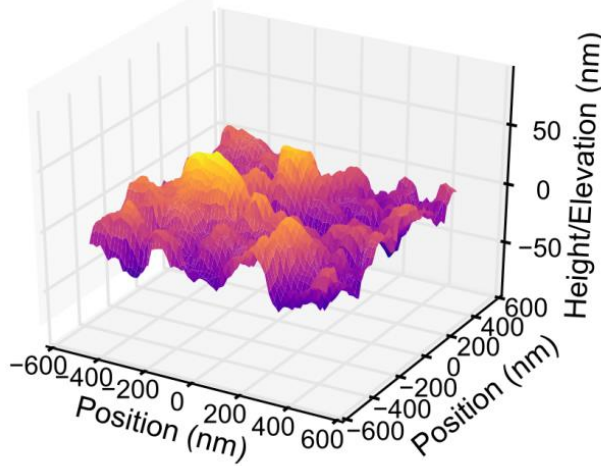
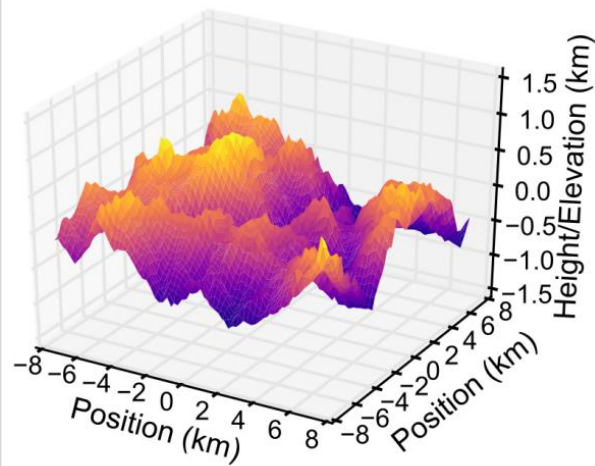
Jacobs, Ryan, Keating, Grierson, Lefever, Turner, Harrison, Carpick, Tribol. Lett. 50, 81 (2013)



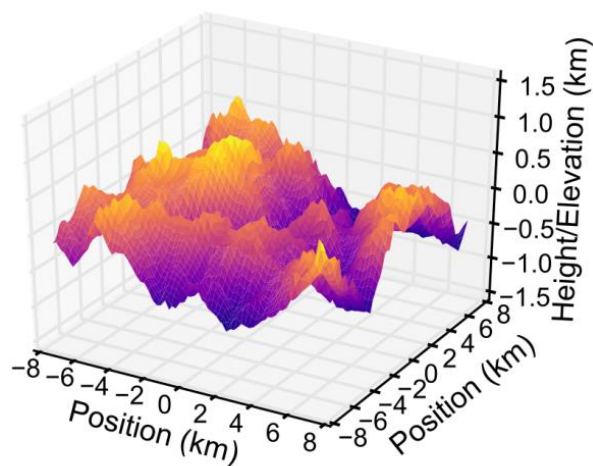
Jacobs, Ryan, Keating, Grierson, Lefever, Turner, Harrison, Carpick, Tribol. Lett. 50, 81 (2013)

Rough surfaces: Structure

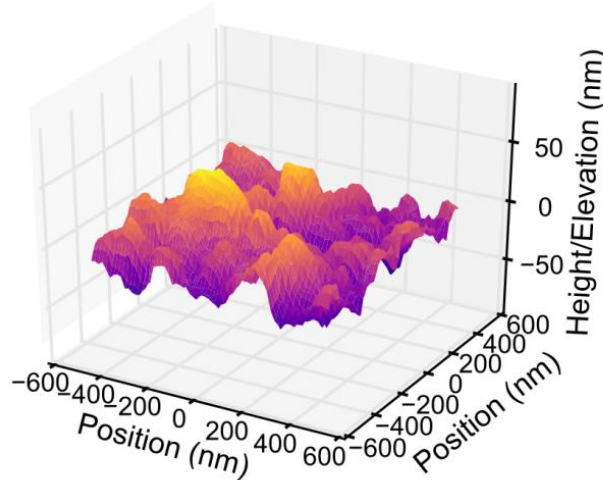




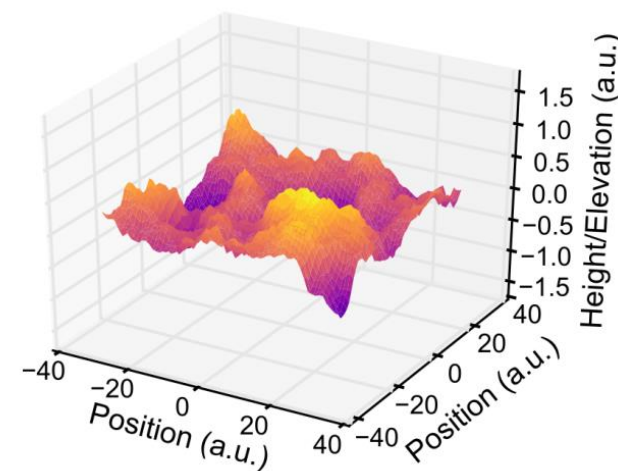
(a) MOUNTAINS



(b) WORN SURFACE



(c) COMPUTER-GENERATED

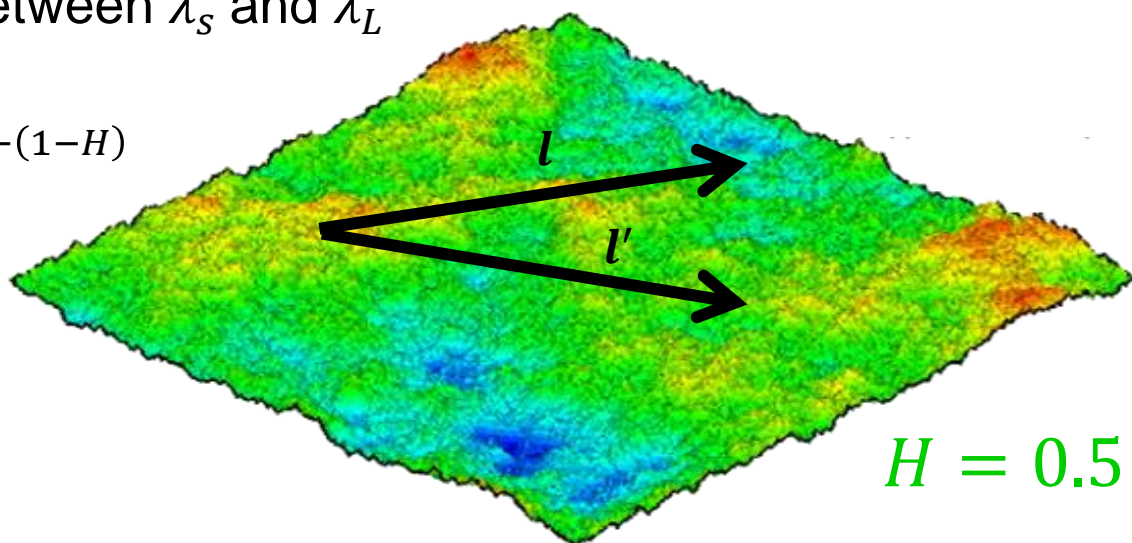


- Height variation dh over length

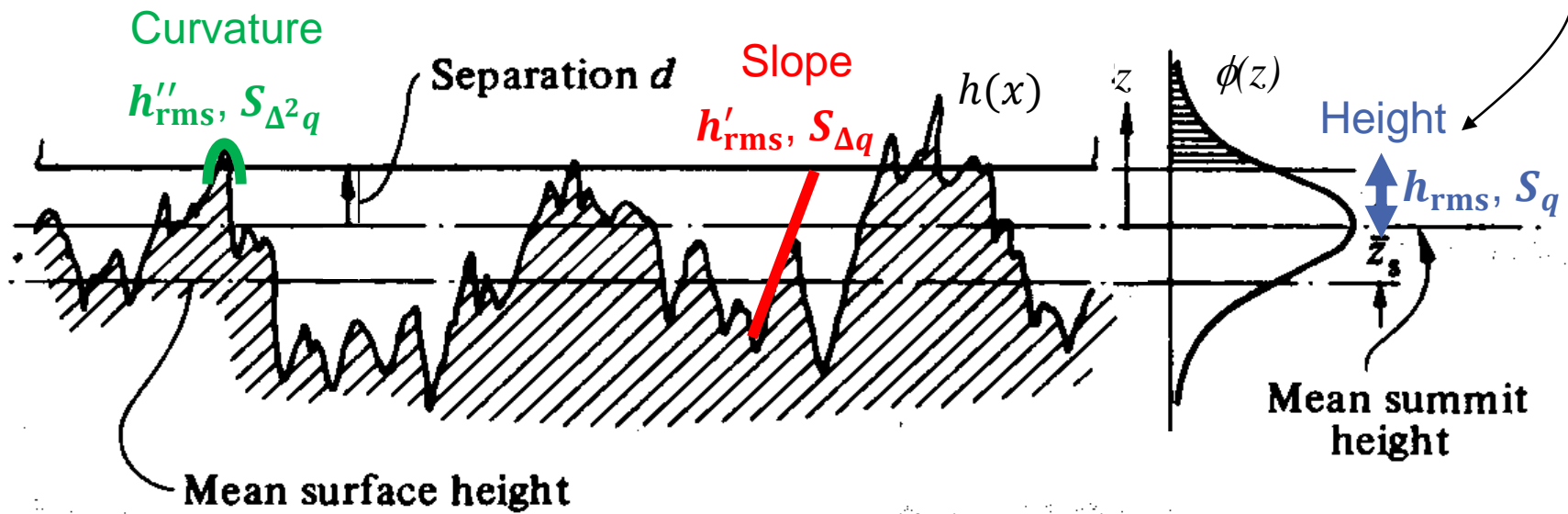
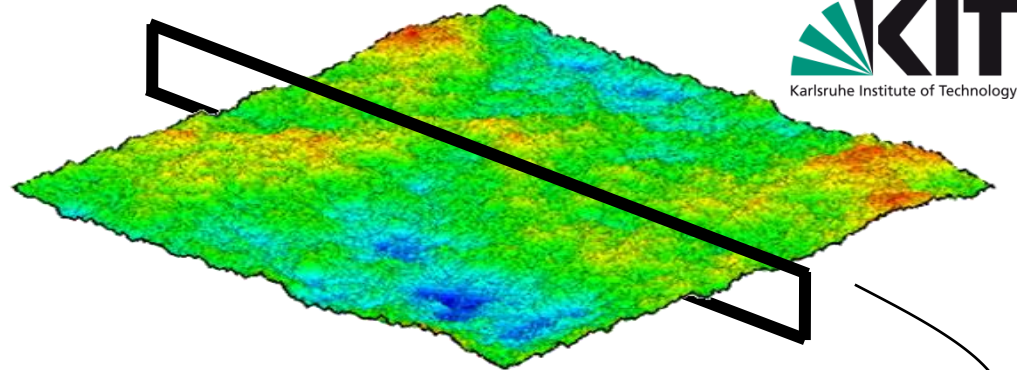
$l \rightarrow dh \propto l^H$ for l between λ_s and λ_L
with $0 < H < 1$

- Average slope $dh/l \propto l^{-(1-H)}$

→ goes to zero
as l increases



Scalar quantities



$$h''_{\text{rms}} = \frac{1}{2} \sqrt{\langle (\nabla^2 h)^2 \rangle}$$

$$h'_{\text{rms}} = \sqrt{\langle |\nabla h|^2 \rangle}$$

$$h_{\text{rms}} = \sqrt{\langle h^2 \rangle}$$

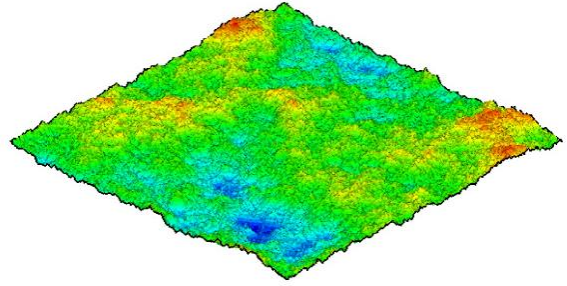
Greenwood, Williamson, *Proc. Roy. Soc. Lond. A* 295, 300 (1966)

Nayak, *J. Lubr. Technol.* 93, 398 (1971)

Greenwood, *Proc. Roy. Soc. Lond. A* 393, 133 (1984)

Correlation functions

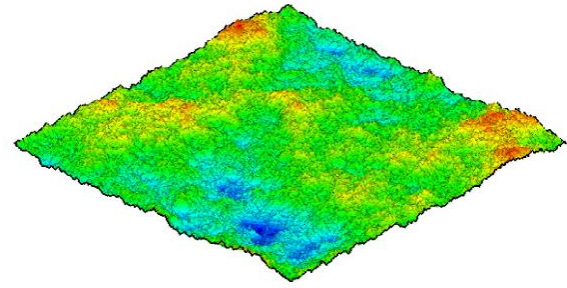
$$h(\vec{x}) = \frac{1}{4\pi^2} \int dq_x dq_y \tilde{h}(\vec{q}) e^{i\vec{q}\cdot\vec{x}}$$



- Height profile

$$h(\vec{x}) \xrightarrow[F]{} \tilde{h}(\vec{q})$$

Correlation functions



$$h(\vec{x}) = \frac{1}{4\pi^2} \int dq_x dq_y \tilde{h}(\vec{q}) e^{i\vec{q}\cdot\vec{x}}$$

- Height profile

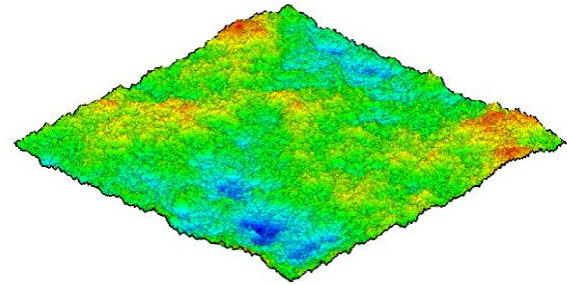
$$h(\vec{x}) \xrightarrow[F]{} \tilde{h}(\vec{q})$$

- Power spectrum

$$\langle h(\vec{x})h(\vec{0}) \rangle \xrightarrow[F]{} C(\vec{q}) = |\tilde{h}(\vec{q})|^2$$

Correlation functions

$$h(\vec{x}) = \frac{1}{4\pi^2} \int dq_x dq_y \tilde{h}(\vec{q}) e^{i\vec{q}\cdot\vec{x}}$$

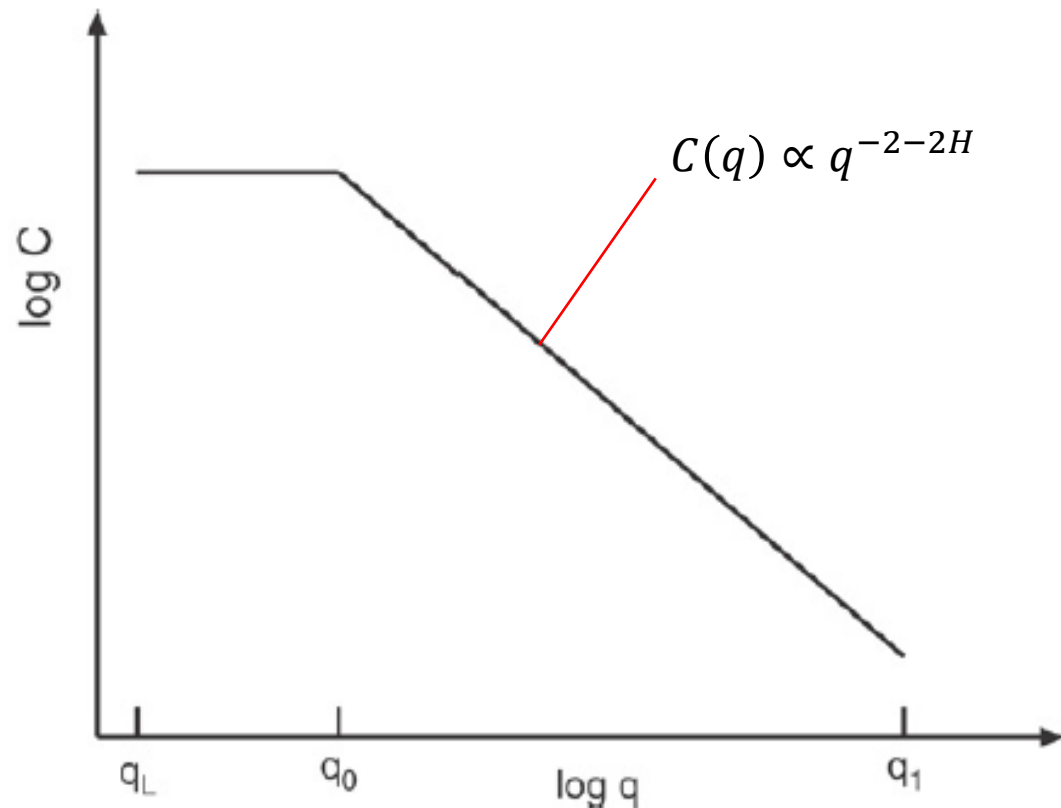


- Height profile

$$h(\vec{x}) \xrightarrow[F]{} \tilde{h}(\vec{q})$$

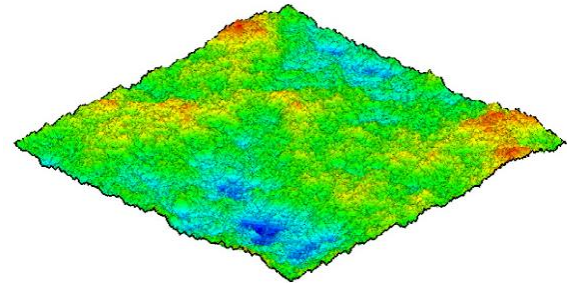
- Power spectrum

$$\langle h(\vec{x})h(\vec{0}) \rangle \xrightarrow[F]{} C(\vec{q}) = |\tilde{h}(\vec{q})|^2$$



Correlation functions

$$h(\vec{x}) = \frac{1}{4\pi^2} \int dq_x dq_y \tilde{h}(\vec{q}) e^{i\vec{q}\cdot\vec{x}}$$

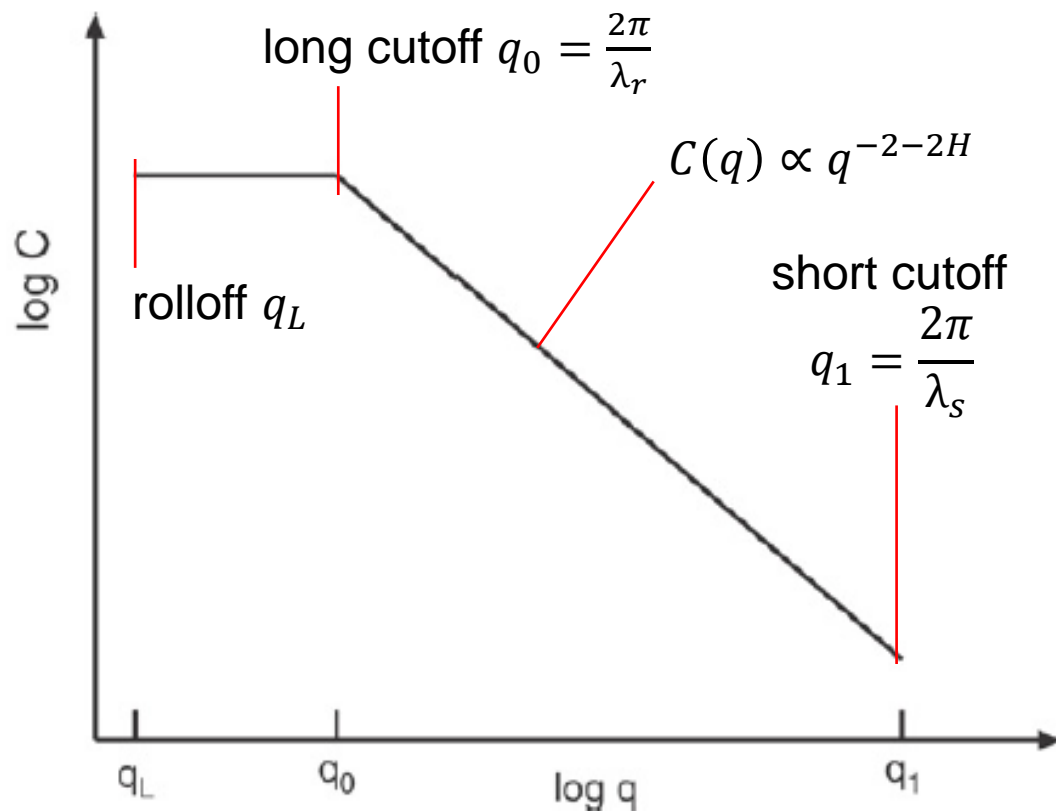


- Height profile

$$h(\vec{x}) \xrightarrow[F]{} \tilde{h}(\vec{q})$$

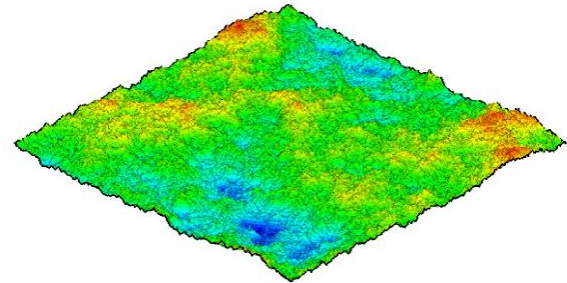
- Power spectrum

$$\langle h(\vec{x})h(\vec{0}) \rangle \xrightarrow[F]{} C(\vec{q}) = |\tilde{h}(\vec{q})|^2$$



Correlation functions

$$h(\vec{x}) = \frac{1}{4\pi^2} \int dq_x dq_y \tilde{h}(\vec{q}) e^{i\vec{q}\cdot\vec{x}}$$



- Height profile

$$h(\vec{x}) \xrightarrow[F]{} \tilde{h}(\vec{q})$$

- Power spectrum

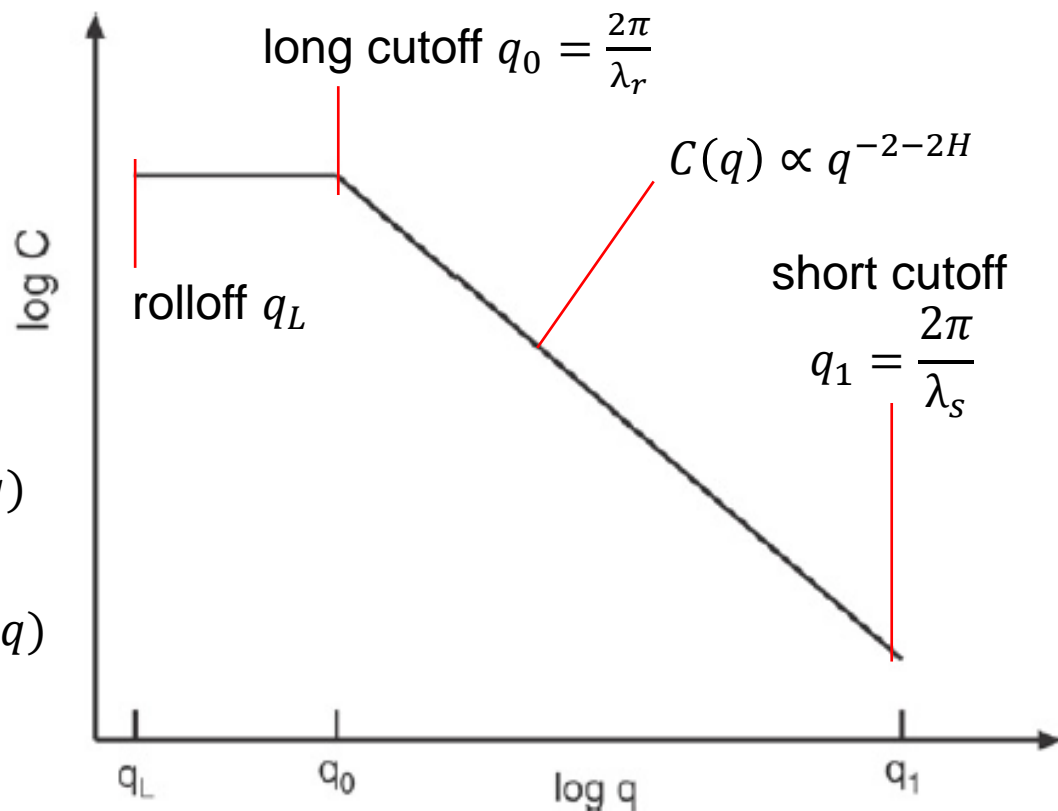
$$\langle h(\vec{x})h(\vec{0}) \rangle \xrightarrow[F]{} C(\vec{q}) = |\tilde{h}(\vec{q})|^2$$

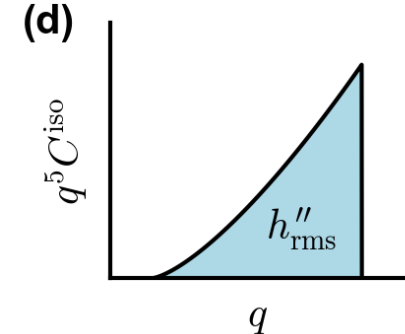
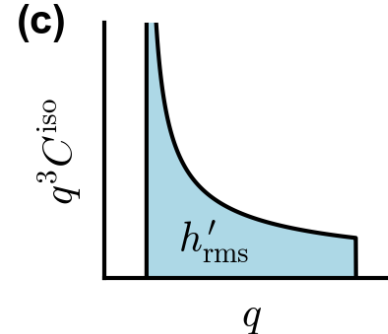
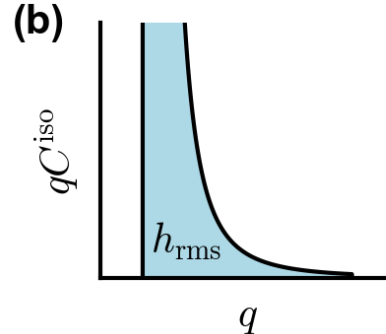
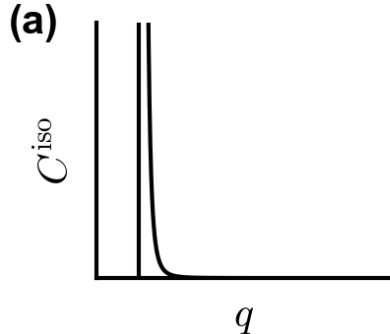
- Sum rules

$$h_{\text{rms}}^2 = \langle |h(x)|^2 \rangle \propto \int dq q C(q)$$

$$(h'_{\text{rms}})^2 = \langle |\nabla h(x)|^2 \rangle \propto \int dq q^3 C(q)$$

$$(h''_{\text{rms}})^2 = \langle |\nabla^2 h(x)|^2 \rangle \propto \int dq q^5 C(q)$$





Jacobs, Junge, Pastewka, Surf. Topogr.: Metrol. Prop. 5, 013001 (2017)

F

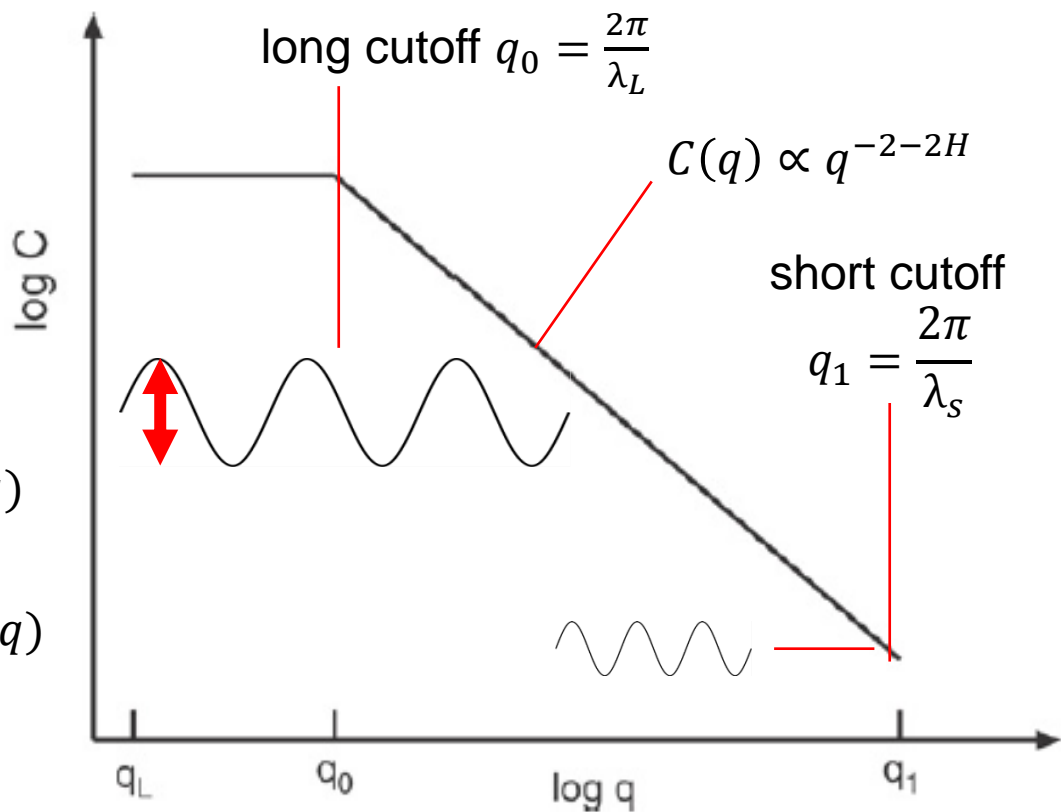
F

■ Sum rules

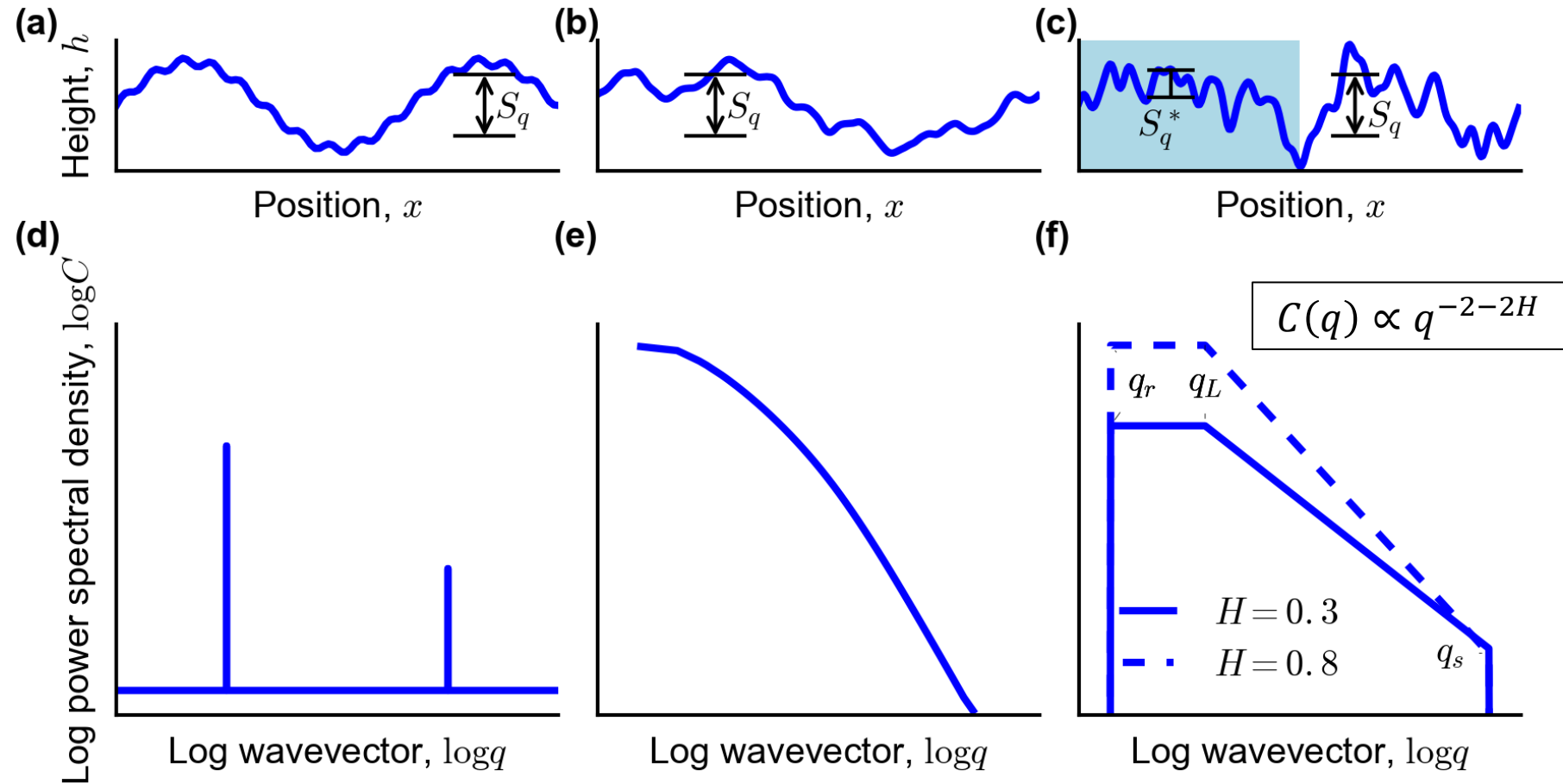
$$h_{\text{rms}}^2 = \langle |h(x)|^2 \rangle \propto \int dq q C(q)$$

$$(h'_{\text{rms}})^2 = \langle |\nabla h(x)|^2 \rangle \propto \int dq q^3 C(q)$$

$$(h''_{\text{rms}})^2 = \langle |\nabla^2 h(x)|^2 \rangle \propto \int dq q^5 C(q)$$

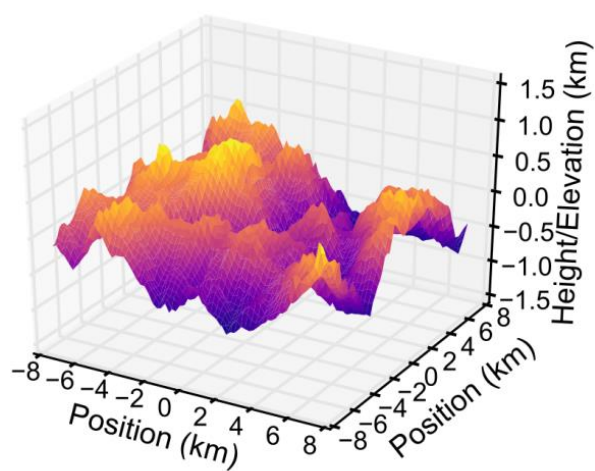


The power-spectral density

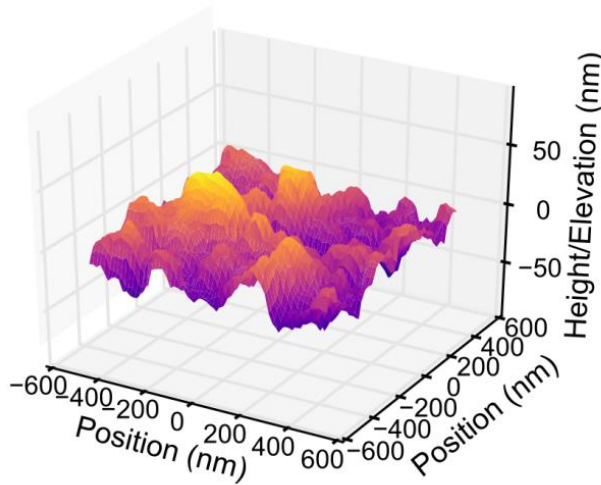


Jacobs, Junge, Pastewka, Surf. Topogr.: Metrol. Prop. 5, 013001 (2017)

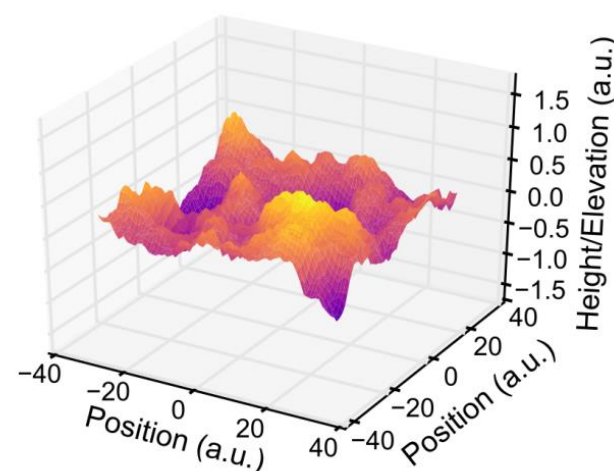
(a) MOUNTAINS



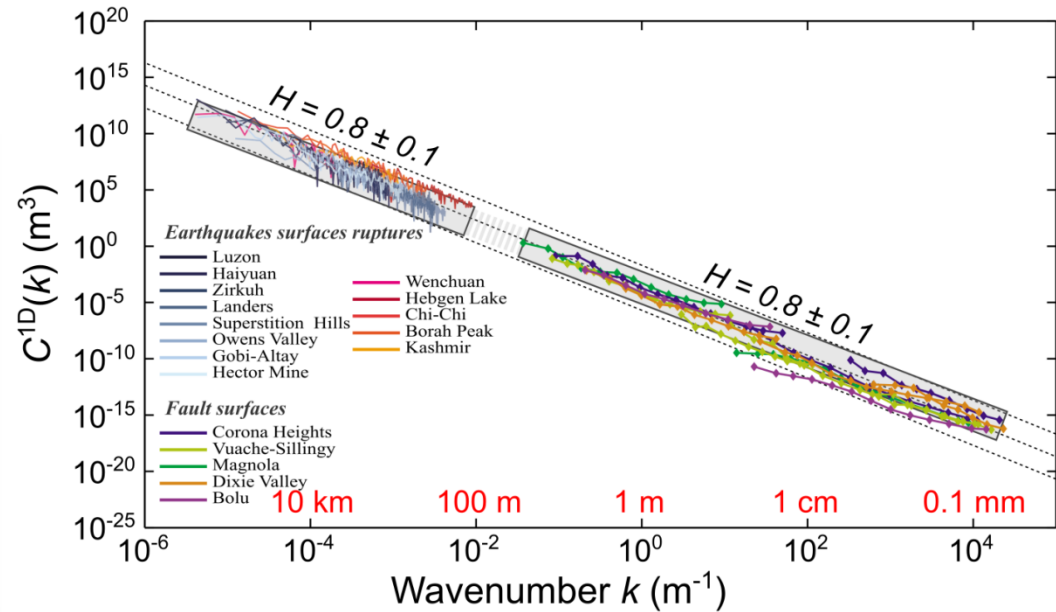
(b) WORN SURFACE



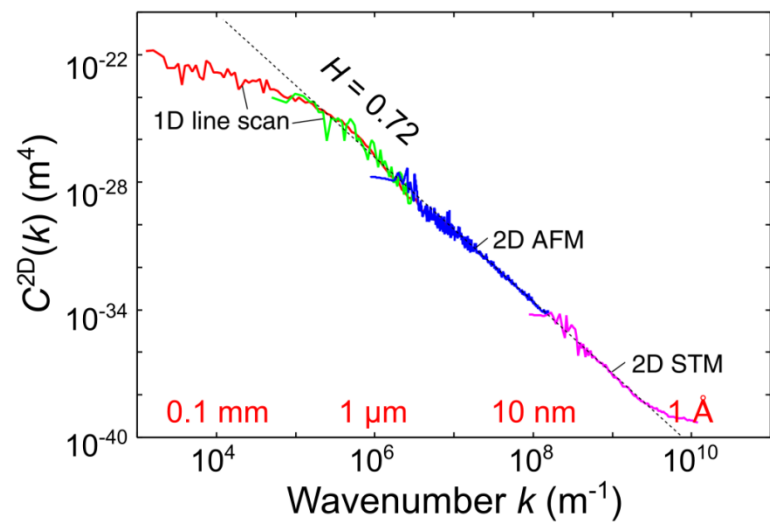
(c) COMPUTER-GENERATED



(d) GEOLOGICAL FAULTS



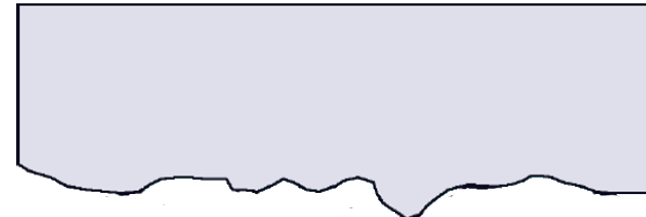
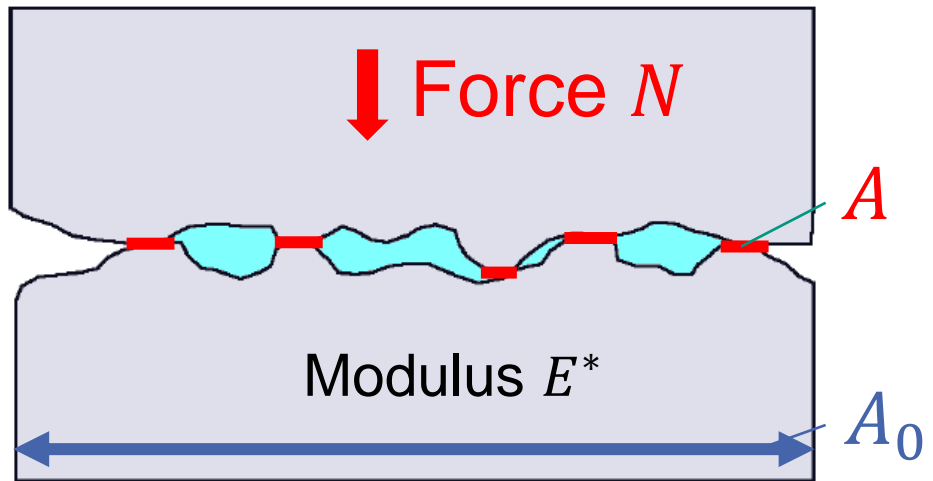
(e) GRINDED STEEL



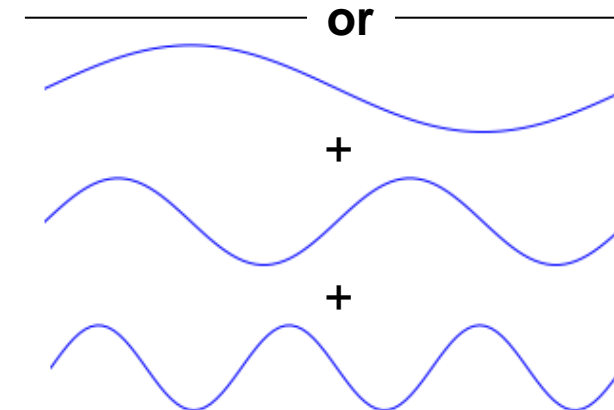
Data from: Candela et al., J. Geophys. Res. 117, B08409 (2012); Persson, Tribol. Lett. 54, 99 (2014); NASA Shuttle Radar Topography Mission; Tevis Jacobs (U. Pittsburgh)

Rough surfaces: Contact

Elastic contact

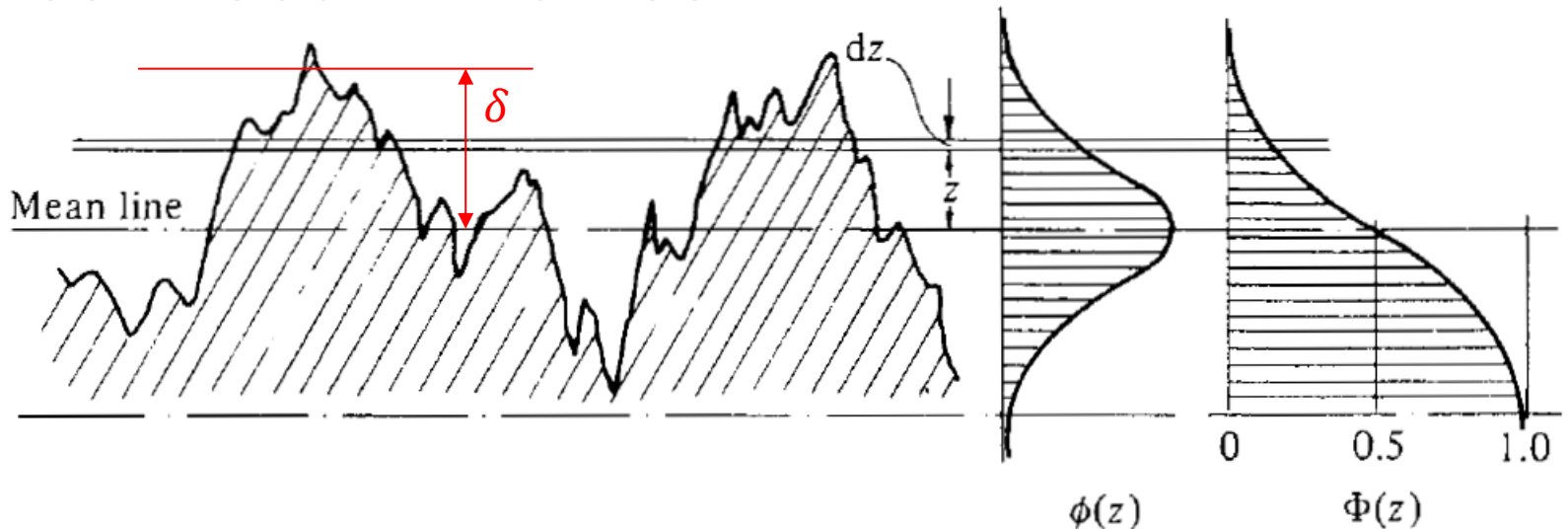


Greenwood-Williamson (1966),
Fuller-Tabor (1975), ...



Longuet-Higgins (1957), Nayak (1971), Persson (2001+), numeric (2004+), ...

Greenwood-Williamson



- Asperity distribution

$$\phi(z) = \frac{1}{\sqrt{2\pi h_{\text{rms}}^2}} \exp\left(-\frac{(z - z_0)^2}{2h_{\text{rms}}^2}\right)$$

Number of asperities

- Number of contacting asperities $n = \int_{\delta}^{\infty} \phi(z) dz$

- Force $\frac{3}{4} \frac{F}{E^* R^2} = n \int_{\delta}^{\infty} \left(\frac{z - \delta}{R}\right)^{3/2} \phi(z) dz$ area $\frac{A}{\pi R^2} = n \int_{\delta}^{\infty} \left(\frac{z - \delta}{R}\right) \phi(z) dz$
- Asperity radius

Greenwood-Williamson

- No closed form solution for Gaussian height distribution
- Height distribution typically approximated as Gaussian, then...

$$\frac{4}{3} \frac{F}{E^* R} = \frac{3\sqrt{\pi}}{4} \frac{n\alpha}{R^{3/2} \lambda^{5/2}}$$

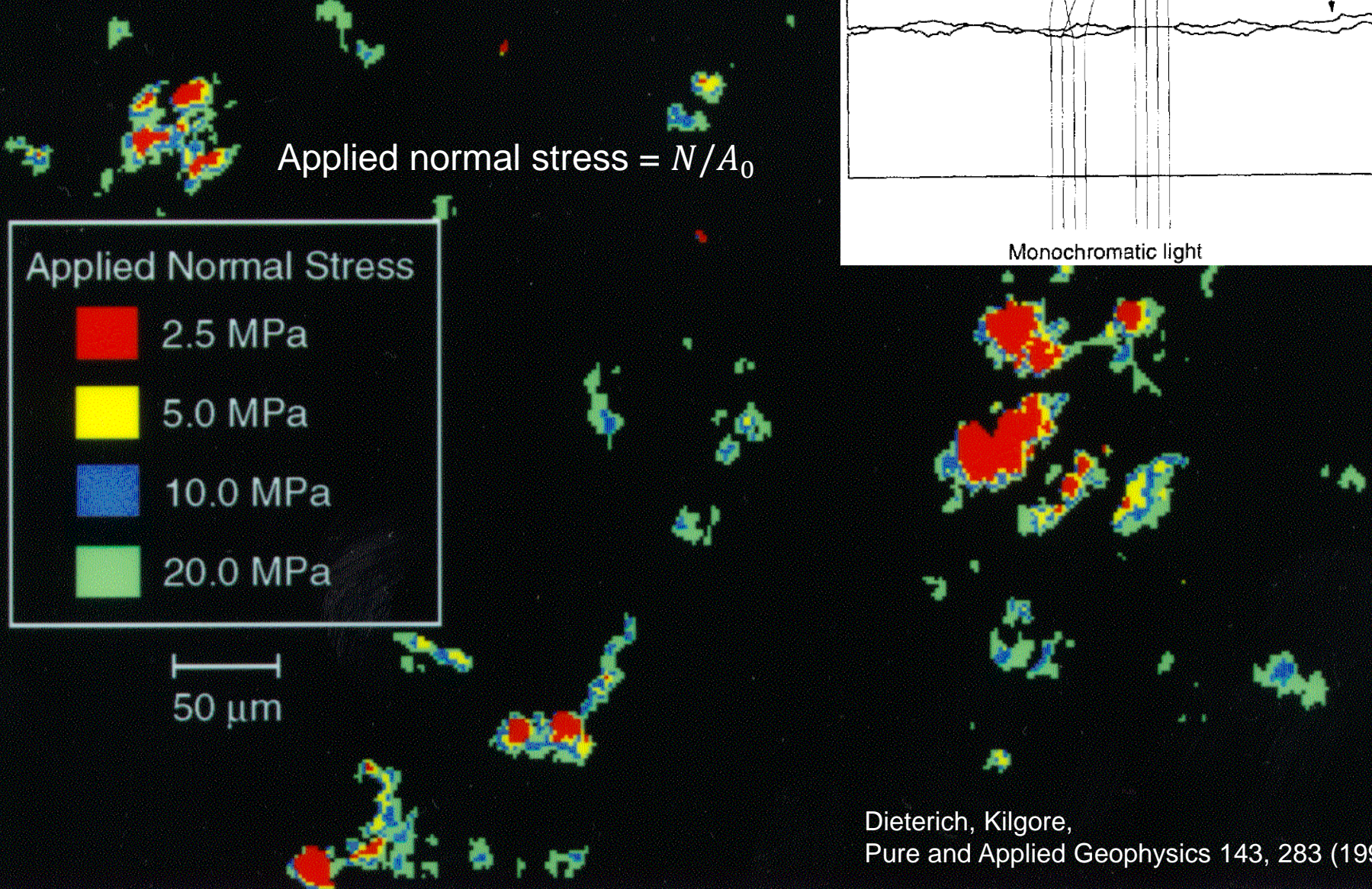
$$\frac{A}{\pi R^2} = \frac{\pi n R \alpha}{\lambda^2}$$

- Ratio of area to load

$$\frac{F}{A} = \left(\frac{3}{4}\right)^2 \frac{E^*}{\sqrt{\pi} (R\lambda)^{5/2}} \quad \text{with} \quad \lambda(\delta) = (\delta - z_0)/h_{\text{rms}}^2$$

- No linearity between area and force

Contact morphology

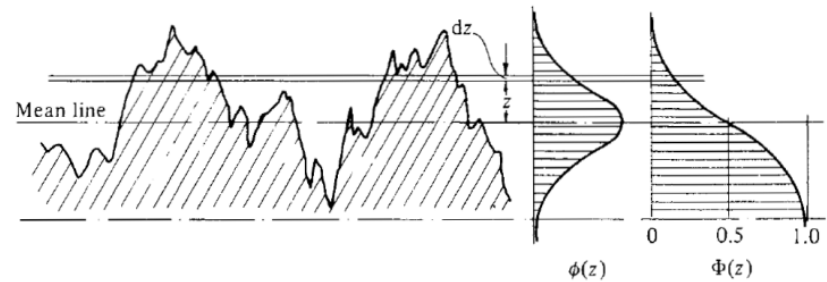


Persson's contact mechanics theory

Persson, J. Chem. Phys. 115, 3840 (2001)

- Simplified argument following Manners & Greenwood [Wear 261, 600 (2006)]
- Assume full conforming contact, i.e. displacement $\bar{u}_z(x, y) \equiv h(x, y)$
- Surface stress and displacement linked by Green's function, diagonal in reciprocal space

$$\tilde{P}(\vec{q}) = \frac{E^*}{2} q \tilde{u}_z(\vec{q}) = \frac{E^*}{2} q \tilde{h}(\vec{q})$$



- The pressure fluctuates locally → compute the standard deviation

$$\langle P^2 \rangle = \frac{1}{A} \int d^2 r P^2(\vec{r}) = \frac{1}{4\pi} \int d^2 q \tilde{P}(\vec{q}) = \frac{E^{*2}}{4} \frac{1}{4\pi^2} \int d^2 q q^2 |\tilde{h}(\vec{q})|^2 = \frac{E^{*2}}{4} h_{\text{rms}}'^2$$

= PSD, $C(q)$

Persson's theory

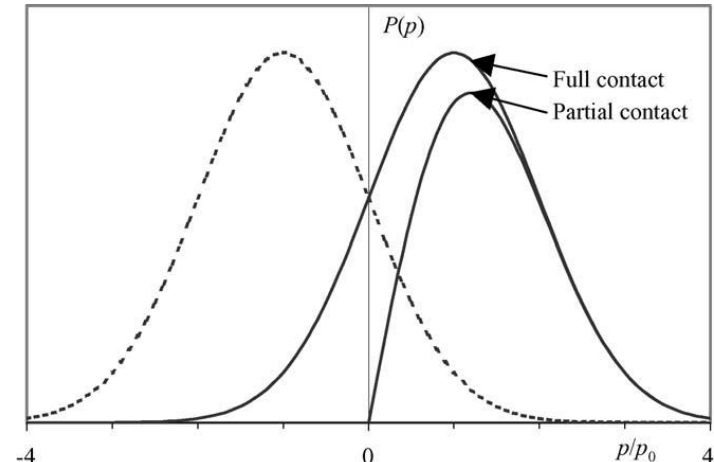
Persson, J. Chem. Phys. 115, 3840 (2001)

- The pressure fluctuates locally

$$\langle P^2 \rangle = \frac{E^{*2}}{4} h_{\text{rms}}'^2$$

- Then (p_0 is applied pressure)

$$P(p, p_0) \propto \exp \left[\frac{(p - p_0)^2}{2\langle P^2 \rangle} \right] = \exp \left[\frac{(p - p_0)^2}{2(h_{\text{rms}}' E^*/2)^2} \right]$$



Manners, Greenwood,
Wear 261, 600 (2006)

- This gives finite probability for negative pressures, cancel with mirror Gaussian

$$P(p, p_0) = \frac{\sqrt{2}}{\sqrt{\pi} h_{\text{rms}}' E^*} \left\{ \exp \left[-\frac{2(p - p_0)^2}{h_{\text{rms}}'^2 E^{*2}} \right] - \exp \left[-\frac{2(p + p_0)^2}{h_{\text{rms}}'^2 E^{*2}} \right] \right\}$$

- Properties

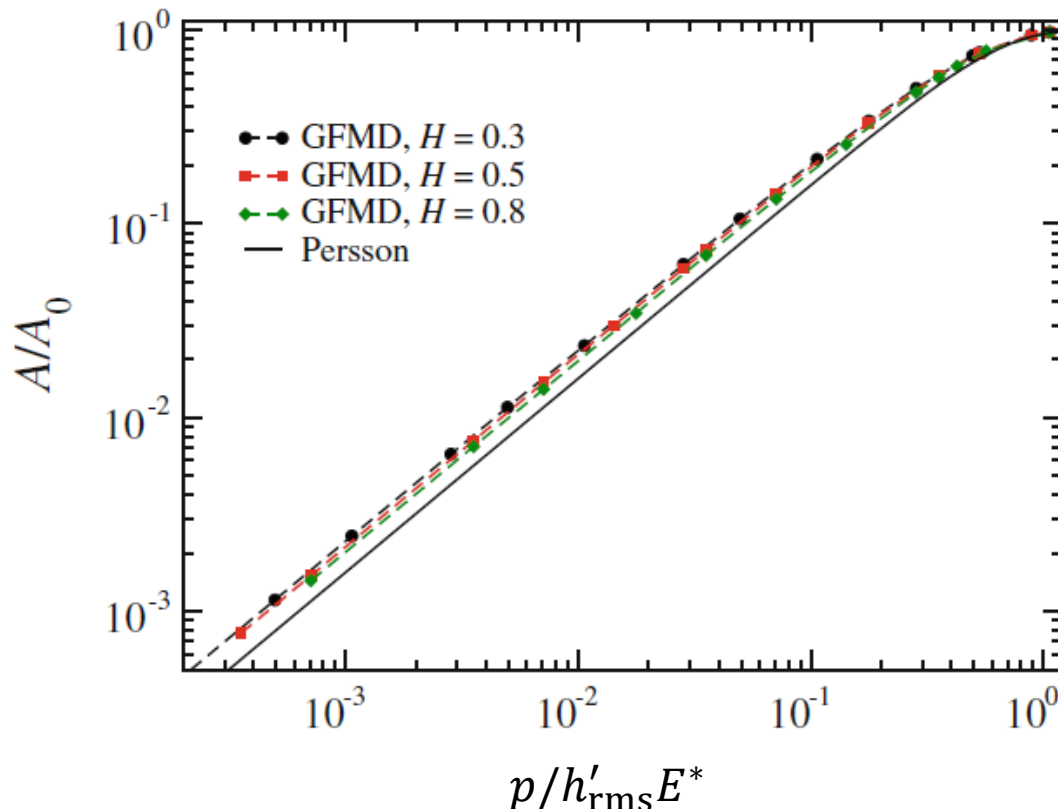
$$\langle p \rangle = \int dp p P(p, p_0) = p_0$$

$$f(p_0) \equiv \frac{A}{A_0} = \int dp P(p, p_0) = \operatorname{erf} \left(\frac{\sqrt{2}p_0}{h_{\text{rms}}' E^*} \right)$$

Persson's theory

Contact area

$$f(p_0) \equiv \frac{A}{A_0} = \int dp P(p, p_0) = \operatorname{erf}\left(\frac{\sqrt{2}p_0}{h'_{\text{rms}}E^*}\right)$$



Prodanov, Dapp, Müser,
Tribol. Lett. 53, 433 (2014)

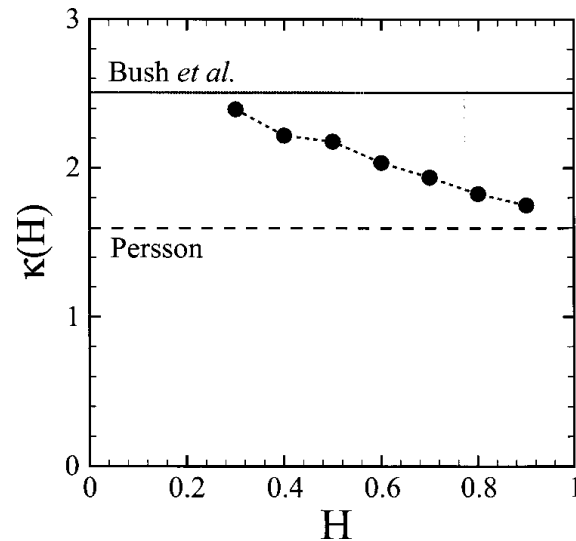
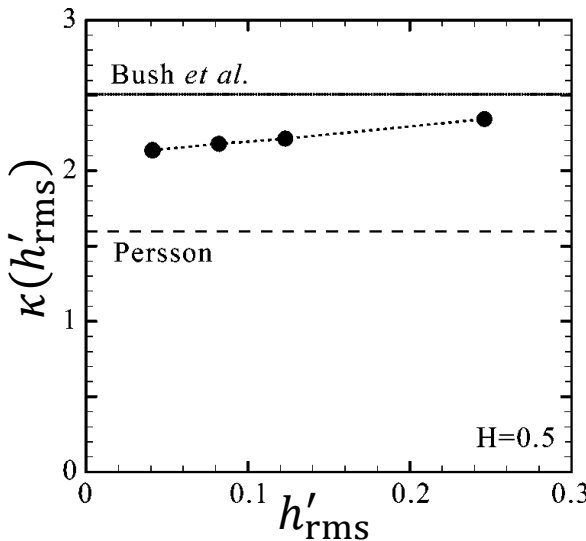
Persson's theory

Contact area

$$f(p_0) \equiv \frac{A}{A_0} = \int dp P(p, p_0) = \operatorname{erf}\left(\frac{\sqrt{2}p_0}{h'_{\text{rms}} E^*}\right)$$

Asymptotic behavior for small p_0

$$f(p_0) = \frac{\sqrt{8}p_0}{\sqrt{\pi}h'_{\text{rms}} E^*} = \frac{p_0}{p_{\text{rough}}} \quad \text{with} \quad p_{\text{rough}} = \frac{h'_{\text{rms}} E^*}{\kappa} \quad \text{and} \quad \kappa = \sqrt{\frac{8}{\pi}}$$

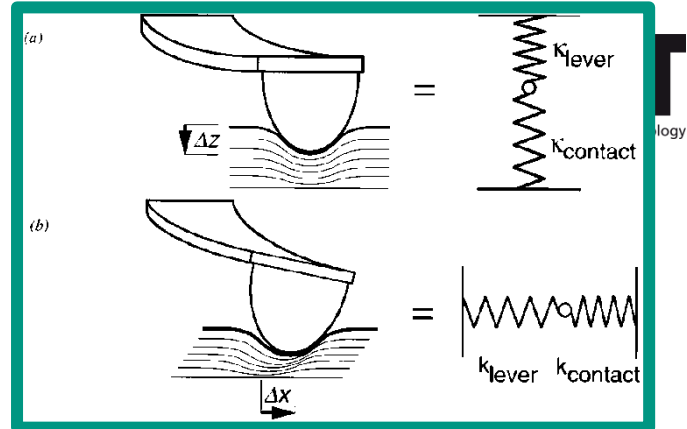
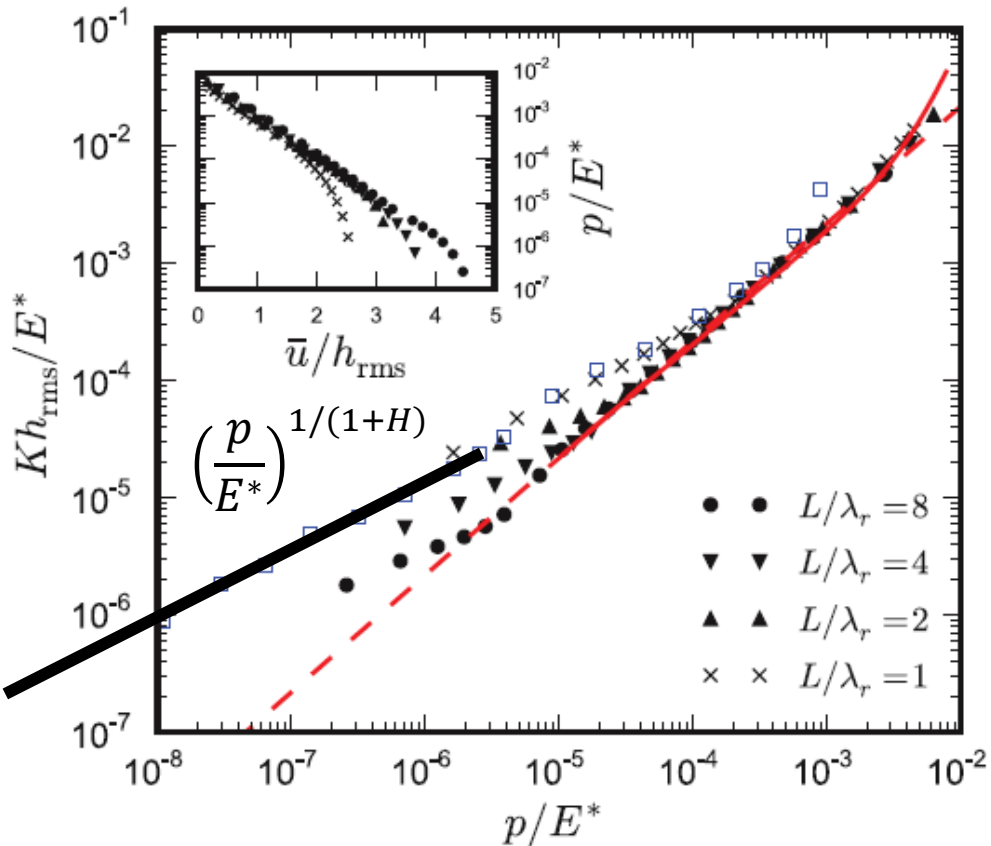


$$\sqrt{2\pi} \approx 2.5$$

$$\sqrt{8/\pi} \approx 1.6$$

Hyun, Pei, Molinari, Robbins,
Phys. Rev. E 70, 026117 (2004)

Contact stiffness $K = dF/d\delta$



- Stiffness proportional to nominal pressure at high load

$$\frac{Kh_{\text{rms}}}{E^*} \propto \frac{p}{E^*}$$

- Power-law at low load

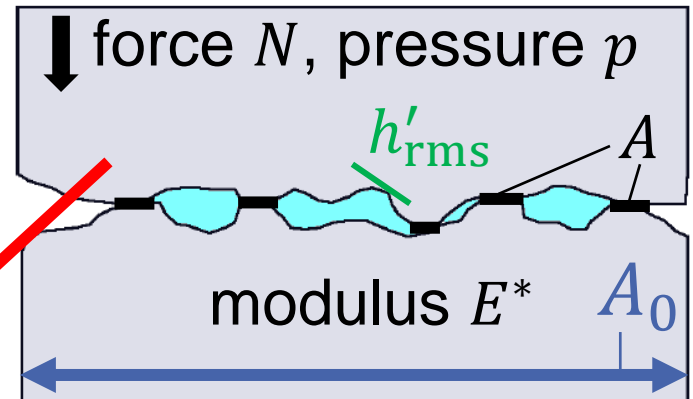
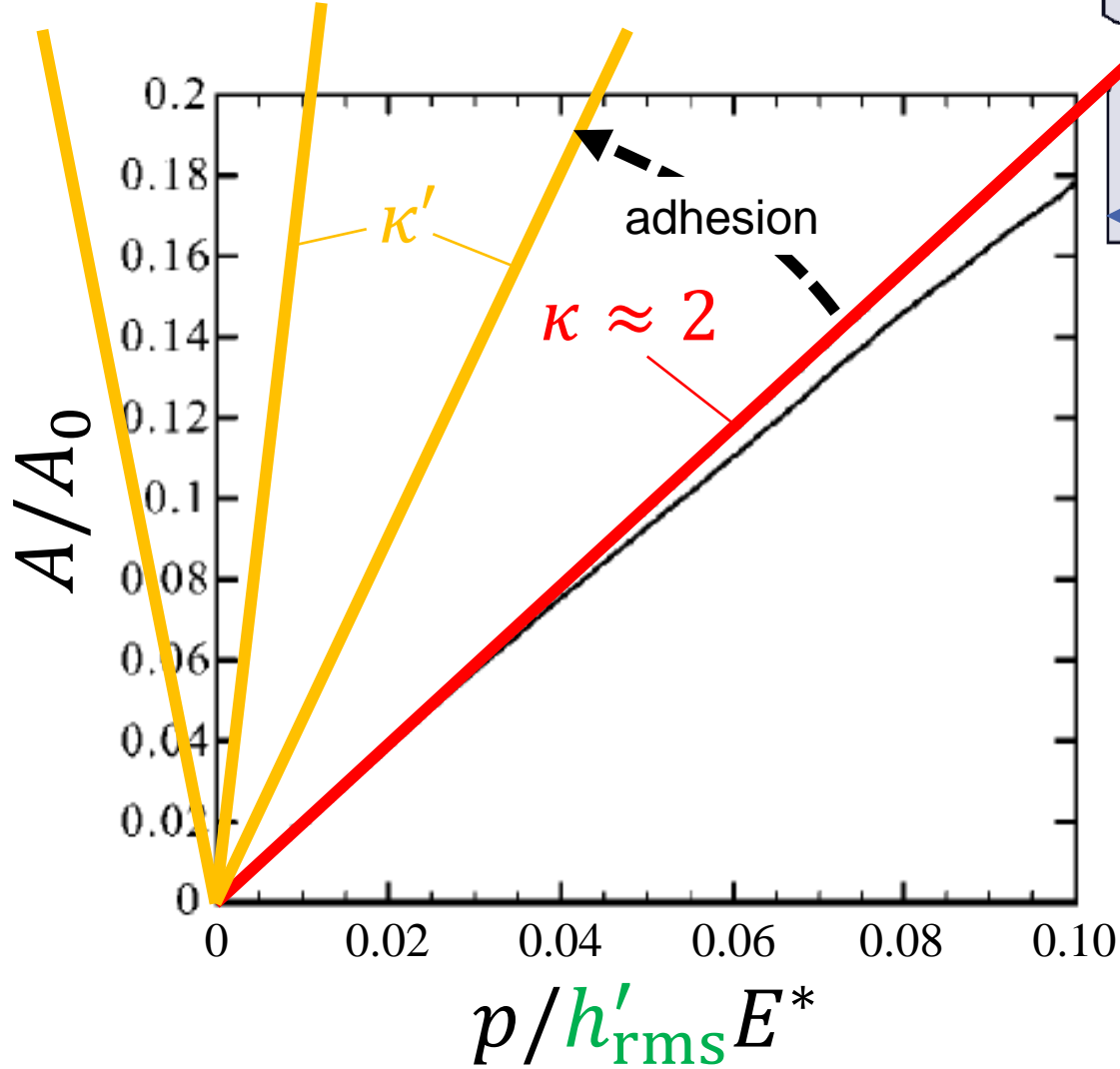
$$\frac{Kh_{\text{rms}}}{E^*} \propto \left(\frac{p}{E^*}\right)^{1/(1+H)}$$

Pastewka, Prodanov, Lorenz, Müser, Robbins, Persson, Phys. Rev. E 87, 062809 (2013)

Pohrt, Popov, Phys. Rev. Lett. 108, 104301 (2012)

Akarapu, Sharp, Robbins, Phys. Rev. Lett. 106, 204301 (2011)

Making contact

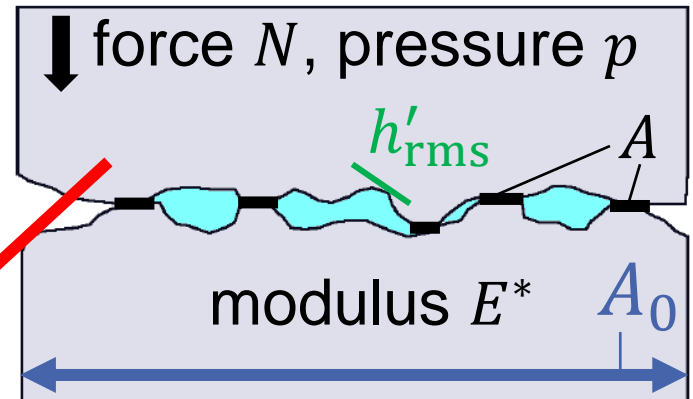
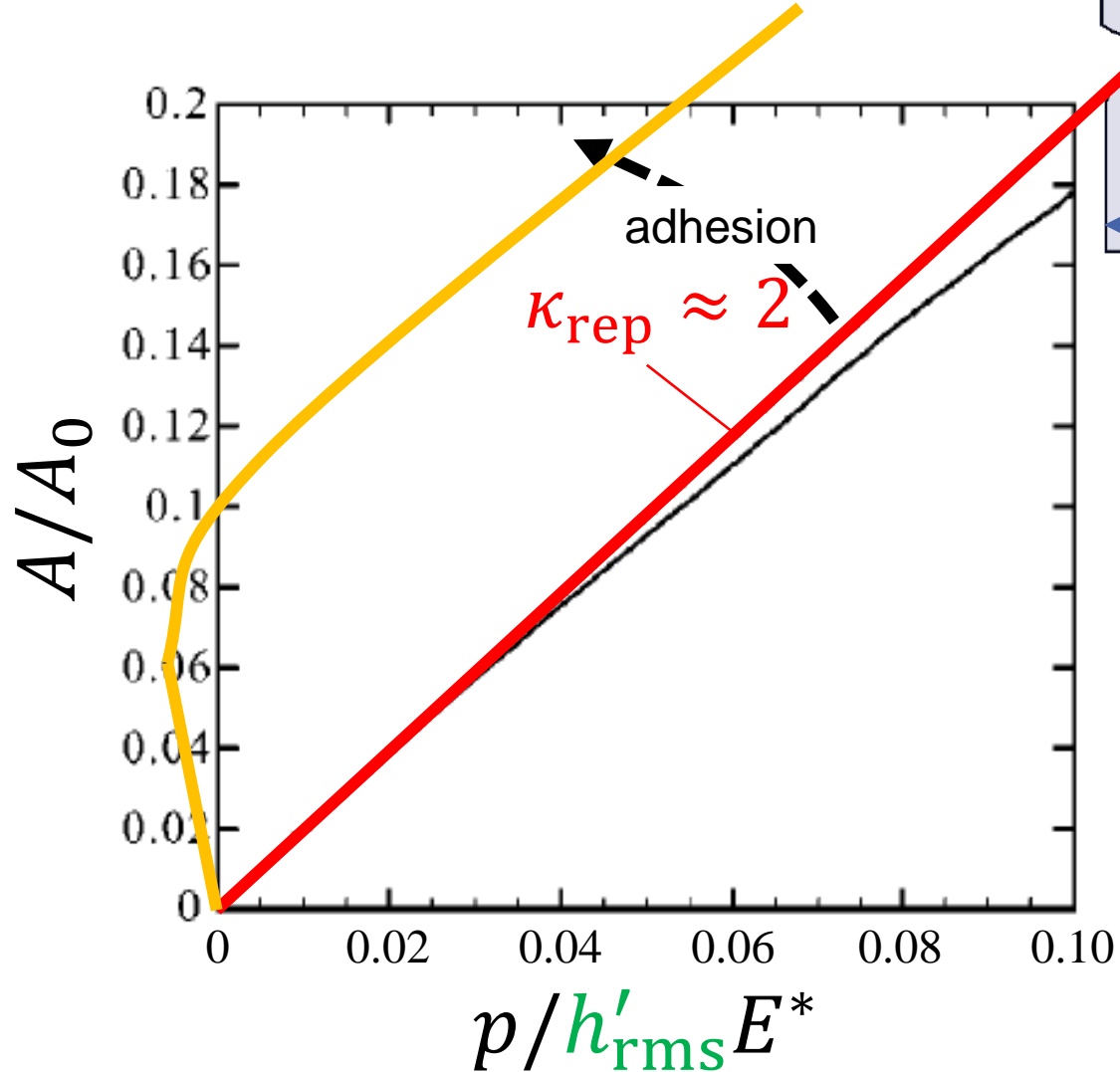


- h'_rms - amplitude of local slope fluctuations
- E^* - elastic contact modulus
- $p = N/A_0$ – nominal pressure

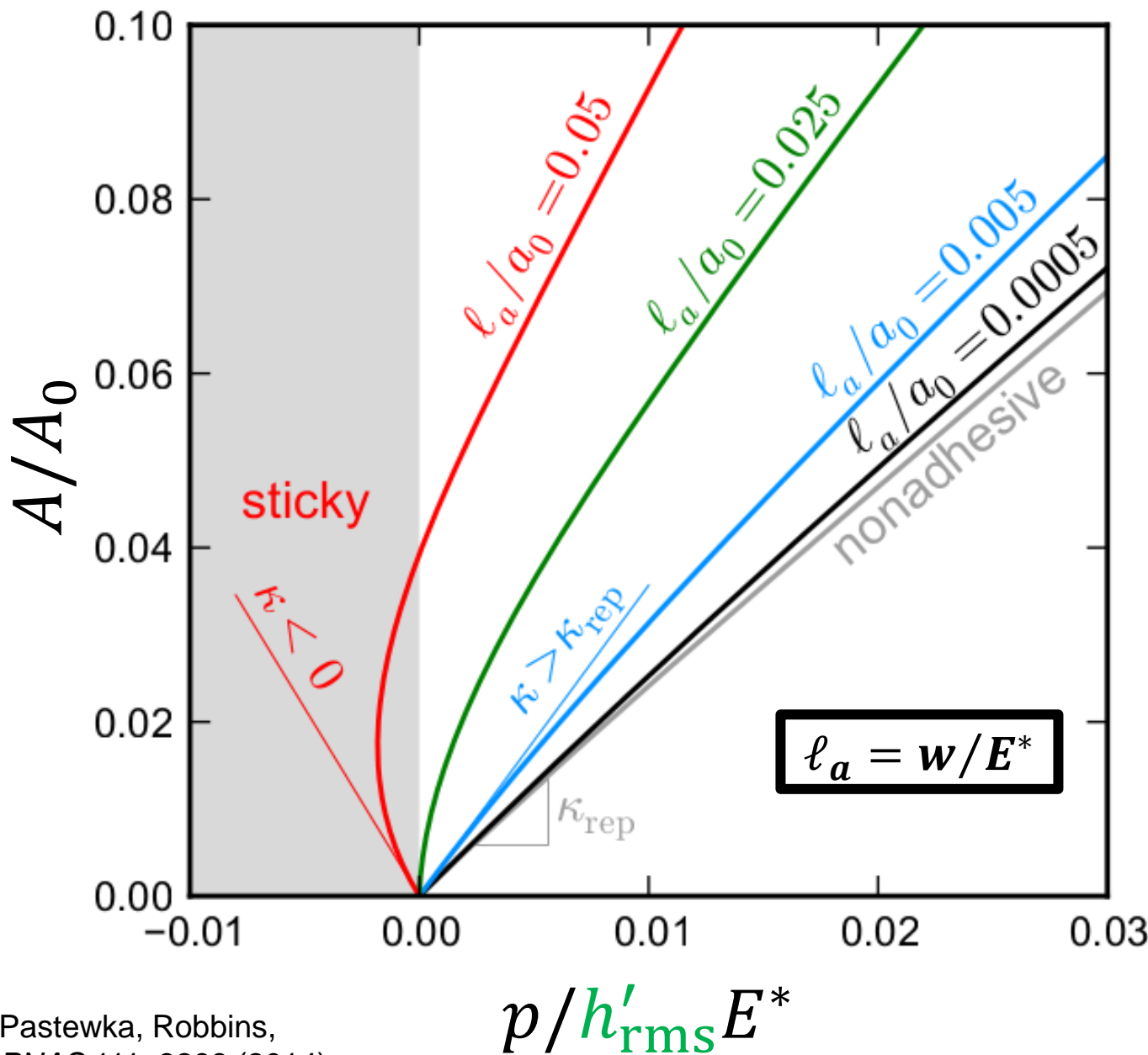
Nonadhesive calculation:
e.g. Hyun, Pei, Molinari, Robbins,
Phys. Rev. E 70, 026117 (2004)

Analytical models:
Bush, Gibson, Thomas, *Wear* 35,
87 (1975); Persson, *J. Chem. Phys.* 115, 3840 (2001)

Adhesive contact



- h'_rms - amplitude of local slope fluctuations
- E^* - elastic contact modulus
- $p = N/A_0$ – nominal pressure



w: work of adhesion
 (energy per unit area gained when bringing flat surfaces in contact)

Pastewka, Robbins,
PNAS 111, 3298 (2014)

Mar. 03, 2017

$$\delta = 0 \quad a_0$$

$$\frac{1}{\kappa} = \frac{N_{\text{rep}} - N_{\text{att}}}{h'_{\text{rms}} E^* A_{\text{rep}}}$$

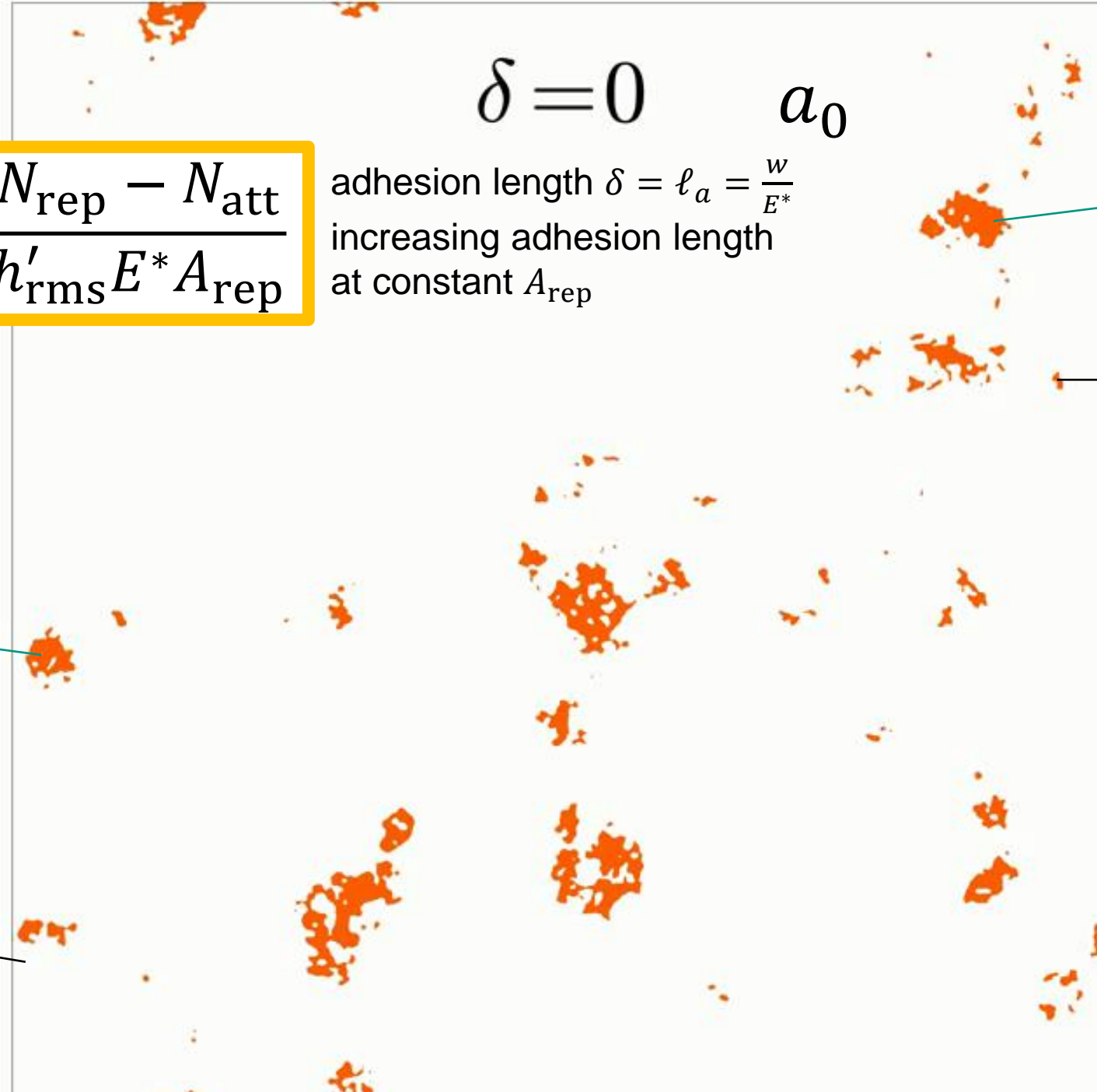
adhesion length $\delta = \ell_a = \frac{w}{E^*}$
increasing adhesion length
at constant A_{rep}

A_{rep}

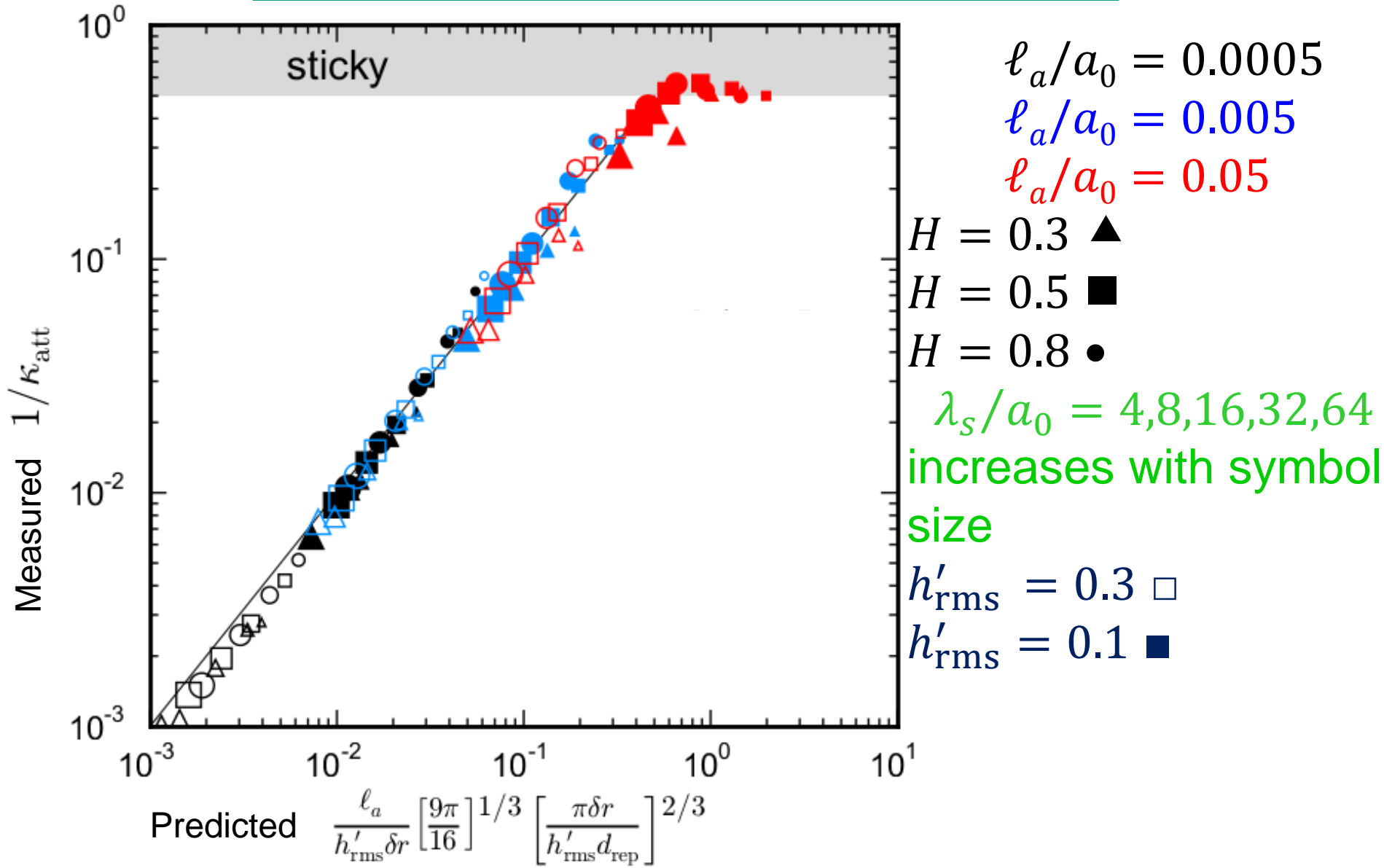
A_{att}

N_{rep}

N_{att}

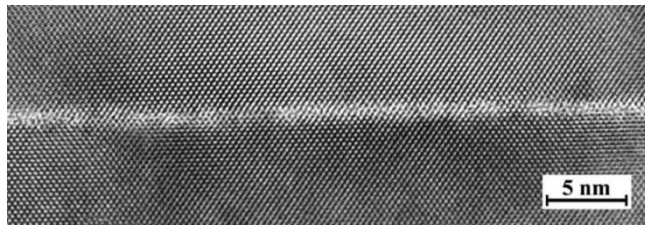


$$N_{\text{rep}} - N_{\text{att}} = \left(\frac{1}{\kappa_{\text{rep}}} - \frac{1}{\kappa_{\text{att}}} \right) A_{\text{rep}} h'_{\text{rms}} E^*$$



Adhesion

Sticky if $\frac{w}{E^* a_0} = \frac{\ell_a}{a_0} \geq 0.5 h'_{\text{rms}}$



Reznicek, Scholz, Senz, Gösele,
Mater. Chem. Phys. 81, 277 (2003)

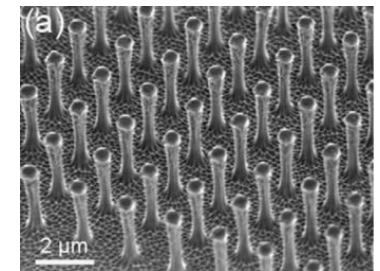
$$h'_{\text{rms}} < 10^{-3}$$



Dahlquist criterion:
 $E^* < 0.1 \text{ MPa}$



Hansen, Autumn,
PNAS 102, 385
 (2005)



Jeong, Suh, *Nano Today*
 4, 335 (2009)

Seals

Dapp, Lücke, Persson, Mäuser,
Phys. Rev. Lett. 108, 244301 (2012)

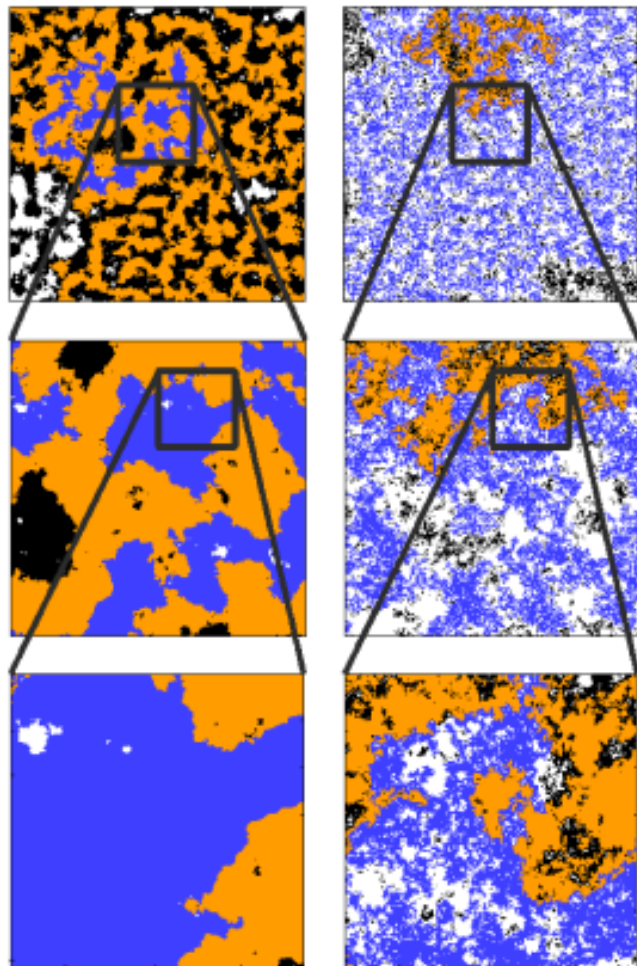


FIG. 1 (color online). Contact and noncontact patches for $A/A_0 = 0.46$ and $H = 0.8$. Black is regular contact, while dark gray (blue) represents the largest connected contact patch. White and light gray (orange) represent similarly noncontact or open channels. Top panels show the full interface. Left: bearing-area model. Right: elastic calculations.

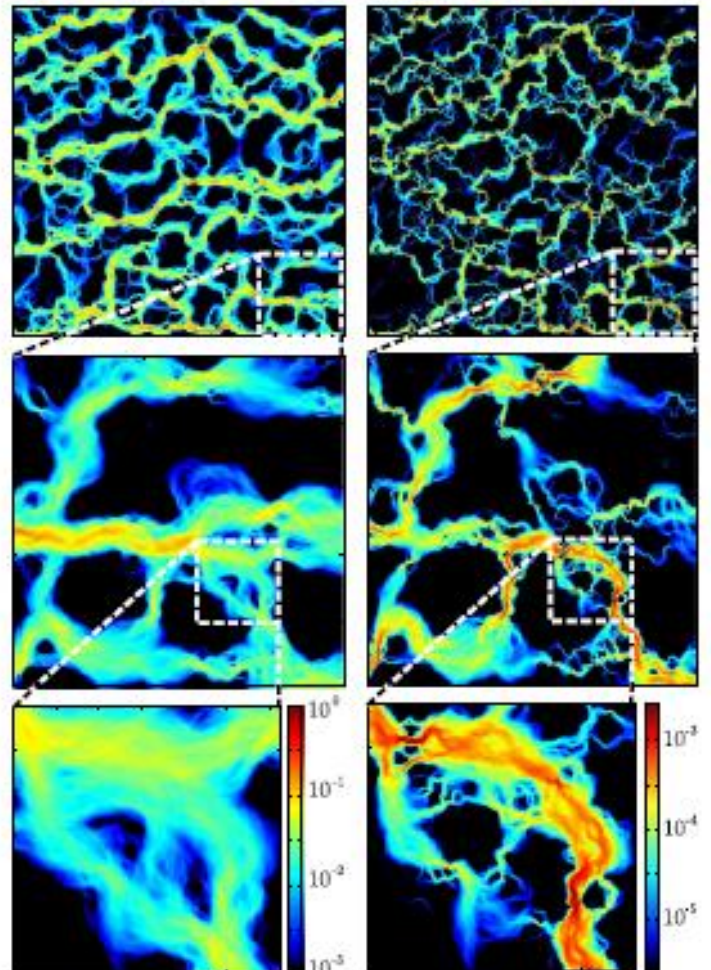
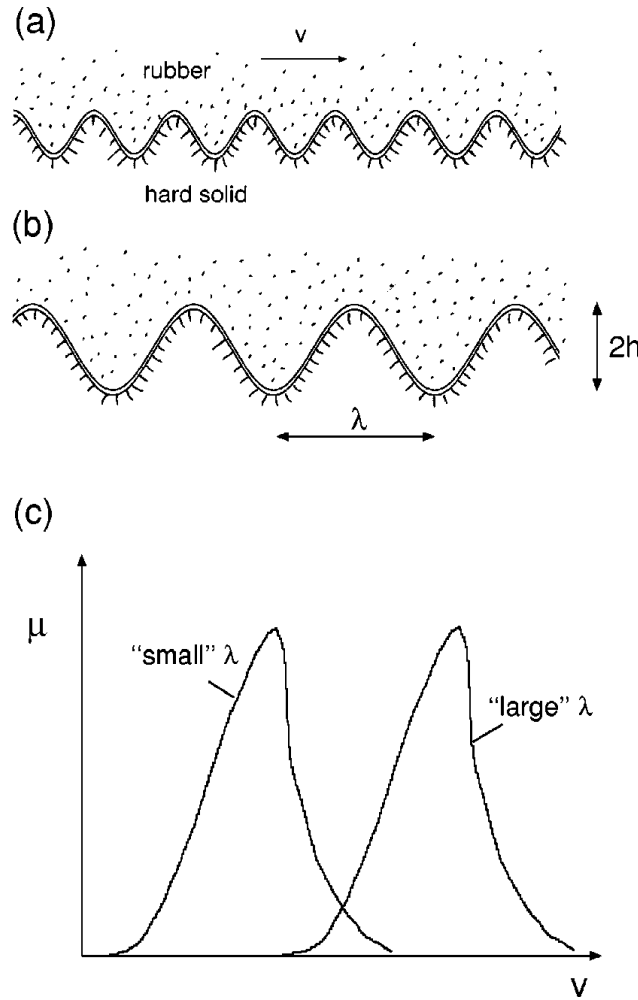


FIG. 2 (color online). Flow density through a contact with $A/A_0 = 0.2$. Left: bearing-area model. Right: elastic calculations. Note that the two scales differ by three decades. While generally the same channels are open, the flow is more constricted in the elastic case. Top panels show the full interface.

Persson's theory for rubber friction

Persson, J. Chem. Phys. 115, 3840 (2001)



- Contact modulus is dependent on excitation frequency

$$\tilde{\vec{P}}(\vec{q}, \omega) = \mathbf{M}(\vec{q}, \omega) \tilde{\vec{u}}_z(\vec{q}, \omega)$$

- Constant sliding velocity \vec{v}

$$\omega = \vec{v} \cdot \vec{q}$$

- This means for contact

$$\tilde{\vec{P}}(\vec{q}) = \mathbf{M}_{\text{eff}}(\vec{q}) \tilde{\vec{u}}_z(\vec{q})$$

- Friction from energy dissipation

$$\Delta E = \int d^2 r dt \dot{\vec{u}} \cdot \vec{P}$$

$$= (2\pi)^3 \int d^2 q d\omega (-i\omega) \tilde{\vec{u}}_z(\vec{q}, \omega) \cdot \tilde{\vec{P}}(\vec{q}, \omega)$$

Persson's theory for rubber friction

Persson, J. Chem. Phys. 115, 3840 (2001)

- Friction from energy dissipation in the bulk

$$\begin{aligned}
 \Delta E &= \int d^2r dt \dot{\vec{u}} \cdot \vec{P} \\
 &= (2\pi)^3 \int d^2q d\omega (-i\omega) \tilde{\vec{u}}_z(\vec{q}, \omega) \cdot \tilde{\vec{P}}(\vec{q}, \omega) \\
 &= (2\pi)^3 \int d^2q d\omega (-i\omega) \tilde{\vec{u}}_z(\vec{q}, \omega) \cdot \mathbf{M}(\vec{q}, \omega) \tilde{\vec{u}}_z(\vec{q}, \omega)
 \end{aligned}$$

- For complete (conforming) contact

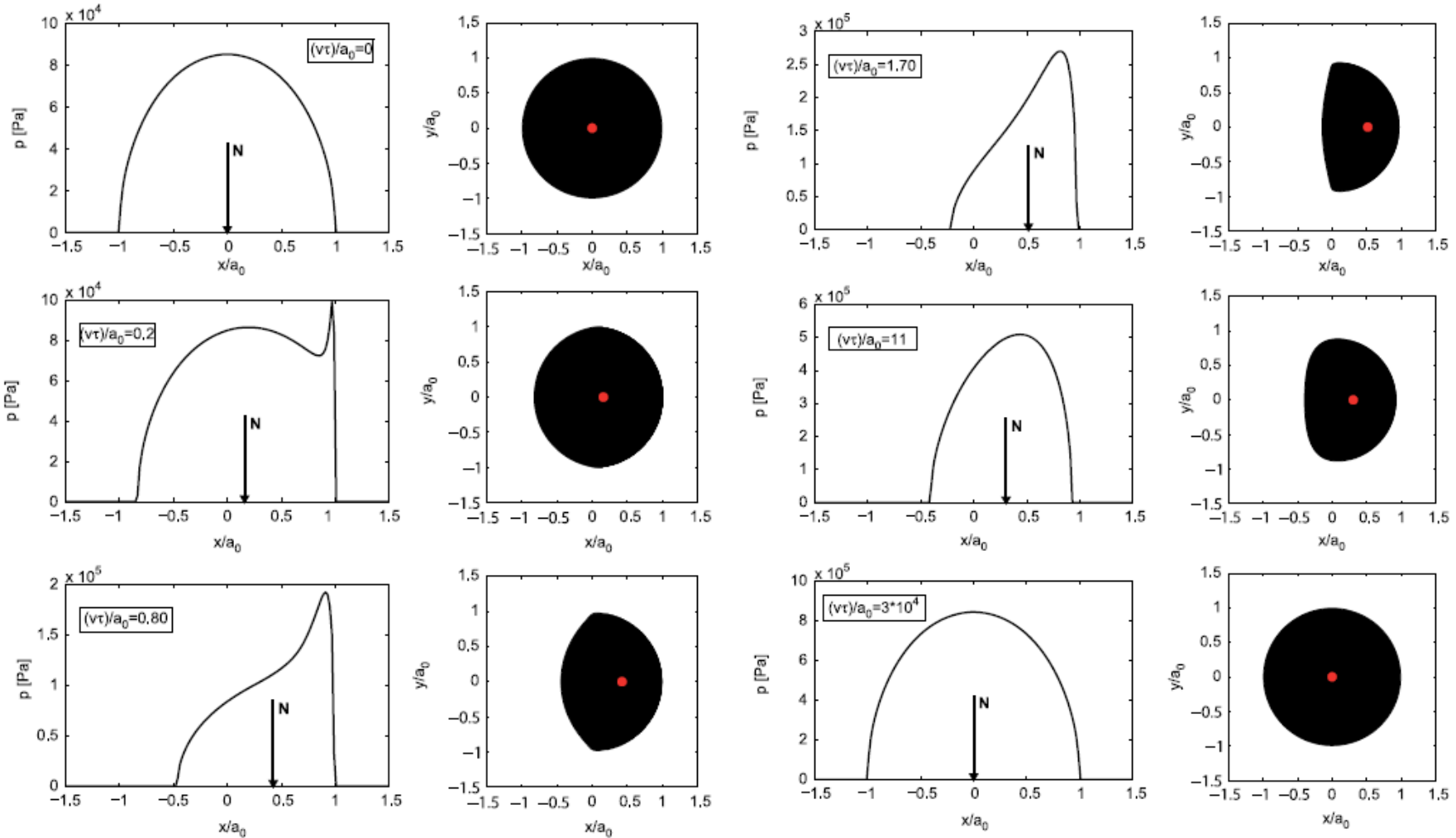
$$\sigma_f = \frac{1}{2} \int d^2q q^2 \cos \phi C(q) \text{Im} \frac{E(q\nu \cos \phi)}{1-\nu^2}$$

- For incomplete contact

$$\sigma_f = \frac{1}{2} \int d^2q q^2 \cos \phi \color{red}{P(q)} C(q) \text{Im} \frac{E(q\nu \cos \phi)}{1-\nu^2}$$

Numerical approaches

$$\mathcal{J}(t) = \mathcal{H}(t) \left[\frac{1}{E_0} - \frac{1}{E_1} \exp(-t/\tau) \right] = \mathcal{H}(t) \left\{ \frac{1}{E_\infty} + \frac{1}{E_1} [1 - \exp(-t/\tau)] \right\}$$

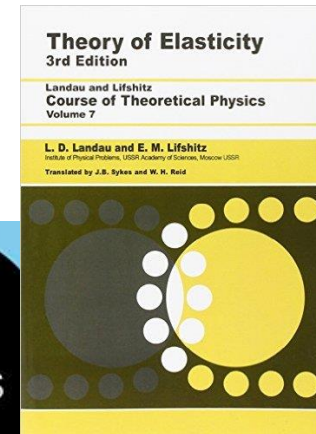


Literature

Theory of Elasticity

Lev D. Landau, Evgeny M. Lifshitz

Butterworth-Heinemann, 3rd edition, 1986



Contact Mechanics

Kenneth Langstreth Johnson

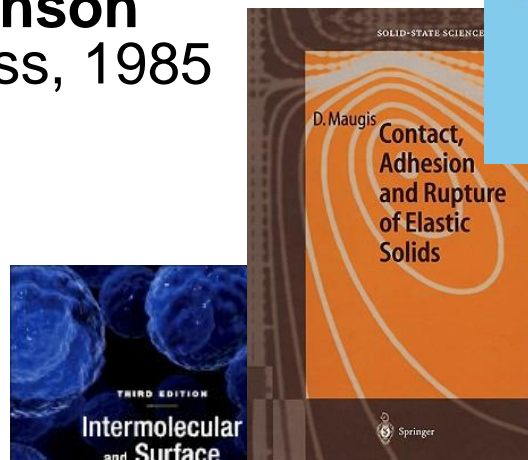
Cambridge University Press, 1985



Contact, Adhesion and Rupture of Elastic Solids

Daniel Maugis

Springer, 2000



Intermolecular and Surface Forces

Jacob N. Israelachvili

Academic Press, 1992

